Numerical Analysis of the Modal Coupling at low resonances in a Colombian Andean Bandola in C using the Finite Element Method

Undergraduate Thesis

Sara E. Rodríguez

srodri13@eafit.edu.co

Thesis Director:

Nicolás Guarín Zapata

Engineering Physics
School of Science and Humanities
Universidad EAFIT
2012

Passing Grade

_____

_____

_____

Presiding Juror

_____

Juror

_____

Juror

_____

Juror

_____

_____

City and Date

Acknowledgements

I would like to thank my supervisor, Nicolás Guarín Zapata, for his advice, patience and support throughout my period of thesis. This work presented owes much to his careful guidance.

I am also grateful to Professor Ricardo Ruiz Boullosa for his enthusiasm and willingness during my experience with acoustics this last year.

I would also like to thank the bandolist Jairo Rincón and the luthiers Luis Arbeláez and Obdulio Velásquez for providing important information about C-Bandola and its musical panorama.

I thank the Applied Mechanics Research Group and also the Research and Teaching Department of Universidad EAFIT, for supporting and providing research facilities.

I am indebted to ANDI association and Universidad EAFIT for funding my undergraduate education. I specially thank Angela Echeverri for her support and advice during my studies.

I thank all the friends and colleagues who have shared the times I have spent as a student.

Finally, I thank all my family. I am grateful to my parents for their love and support in every crazy idea.

Summary

The work presented in this thesis is concerned with the dynamical behavior of a C-Bandola's acoustical box at low resonances. Two models consisting of two and three coupled oscillators are proposed in order to analyse the response at the first two and three resonances, respectively. These models describe the first resonances in a bandola as a combination of the lowest modes of vibration of enclosed air, top and back plates. Physically, the coupling between these elements is caused by the fluid-structure interaction that gives rise to coupled modes of vibration for the assembled resonance box. In this sense, the coupling in the models is expressed in terms of the ratio of effective areas and masses of the elements which is an useful parameter to control the coupling.

Numerical models are developed for the analysis of modal coupling which is performed using the Finite Element Method. First, it is analysed the modal behavior of separate elements: enclosed air, top plate and back plate. This step is important to identify participating modes in the coupling. Then, a numerical model of the resonance box is used to compute the coupled modes. The computation of normal modes of vibration was executed in the frequency range of 0-800Hz. Although the introduced models of coupled oscillators only predict maximum the first three resonances, they also allow to study qualitatively the coupling between the rest of the computed modes in the range.

Considering that dynamic response of a structure can be described in terms of the modal parameters, this work represents, in a good approach, the basic behavior of a C-Bandola, although experimental measurements are suggested as further work to verify the obtained results and get more information about some characteristics of the coupled modes, for instance, the phase of vibration of the air mode and the radiation efficiency.

Contents

List of Figures

7

Glossary

- **Bandola's C tuning:** It is the tuning for the bandola in which its music notation agrees with the real pitch of the equal tempered scale.

- **Bandola's B♭ tuning:** It is a transposing tuning in which musical notes on the bandola produce one tone bellow of the real pitch in the equal tempered scale, therefore, the musical notation is written one tone above the considered pitch.

- **Estudiantina:** It is a type of musical group common in the South American Andean Region. It is formed only by strings instruments which usually are native of the region, for instance, bandolas, tiples, requintos, among others.

- **Mobility:** . It is a measure of the dynamical response of a system. It is expressed as the ratio between velocity and the applied force.

- **Normal mode of vibration:** It is an inherent property of a system in which all the points moves with the same frequency and reaches their maximum or minimum positions at the same time.

- **Open strings:** It refers to the sound generated by the string when it is plucked without frets being pressed.

- **Plucked String Instruments:** These instruments are a subcategory of string instruments. They are played by plucking or exciting the strings with either a finger or a plectrum.

- **Resonance:** Is a state of a system in which all the energy is used to vibrate, thus, even small periodic driving forces can produce large amplitude oscillations.

- **Sound Register:** It indicates the frequency range of the sound produced with the musical notes of an instrument.

Introduction

International research in the field of acoustics is becoming and is playing an important role in the great advances occurring in the scientific, commercial and cultural fields. This increasing participation can be seen in many applications such as musical production, noise reduction and Research and Development of musical instruments. However, this scenario is not very common in Colombia, especially in the field of musical acoustics, where the majority of instruments belonging to our culture are still empirically built [1].

The Colombian Andean Bandola is a musical instrument that experienced a parallel development in many places and which currently presents different regionalized design adaptations. Given these conditions, it is not possible to identify a standard Colombian Andean Bandola, not even a single characteristic sound or tuning [1]. The differences lie in the ways in which instruments are built by regional luthiers and this fact, together with reforms recently proposed by musicians and luthiers from Bogota savannah, have led to a discussion about the identity of the instrument with respect to its sonority and national musical tradition [1].

Research on the acoustics of musical instruments has attempted to relate physical parameters with the characteristic sound of an instrument [6–32]. For this purpose, some phenomena, mainly in the sound production and propagation, are studied based on the behavior of the instrument. The first important application of musical acoustics was done to violins and guitars [6–32]. The study of these instruments provided useful information to luthiers about parameters that could modify the acoustical response of the instrument. In this sense, this work studies, using the finite element method, the normal modes of vibration for the Colombian Andean C-Bandola. Normal modes are well known acoustic parameters which describe the vibrational response of the instrument. The bandola could be understood as a complex mechanical system, whose dynamic behavior depends largely on the interaction and coupling of each of its constituent elements. Knowledge about the dynamic characteristics of resonance box

elements can give an idea of how structural parameters influence the behavior of the instrument as a whole. The analysis of modal coupling at the resonance box is thus proposed and developed throughout the document.

The methodology and results were validated based on reported studies, primarily of guitars. The analysis at low resonances is emphasized through two models consisting of coupled oscillators, which could represent the vibrations of enclosed air, top and back plates at their lowest resonances. The approach of a thesis on this topic is intended not only contributions in academia, but also potential cultural impacts.

Chapter 1

Project Statements

1.1   General Objective

Analyse using FEM the modal coupling at low frequencies of the Colombian Andean C-Bandola's constitutive elements

1.2   Specific Objectives

- Know different reported numerical models for simulating string instruments similar to the bandola.

- Evaluate models and conditions that allow the dynamic behavior description of Colombian Andean C-Bandola.

- Define the numerical model that will be used, the constitutive elements to consider, the material characteristics and boundary conditions.

- Model using CAD software the instrument constitutive elements and the assembled structure.

- Simulate individual modal behavior of elements involved on model dynamic response and also their modal coupling.

- Analyse results and compare them qualitatively with experimental, analytical and numerical reported results for string instruments similar to the bandola.

1.3   Justification

The Colombian Andean Bandola is a plucked string instrument whose origins date back 200 years and which nowadays presents different designs according to two main tunings, B♭ and C. Although the use of the C-Bandola is relatively new (established in 1961), its development in recent years has been thought to make up for some functional shortcomings of the B♭-Bandola. Variations, primarily in size, type and number of strings, are meant to expand interpretation possibilities. The C-Bandola has come to be widely accepted and used by those *estudiantina* types of musical groups, and thus, it have began to be of interest to players and luthiers. Moreover, musical acoustics has led and increase in knowledge of the physical behavior of different musical instruments, particularly in sound production, and it has identified some important parameters that influence the characteristic sound of each instrument. A group of fundamental parameters turns out to be the modes of vibration of the instrument, which are related to particular conditions of sound production since each of them excites the surrounding air in a specific way.

Knowing some information about these modes, one could completely determine the dynamics of a structure. This could be done based on the developed experimental modal analysis techniques, which seek to obtain the modal parameters consisting of frequency, damping and modal shapes. However, these techniques involve specialized devices and assemblies that are complex and have high costs, and hence, are not always available. Computational methods emerge as alternative techniques that provide a predictive capability and can be used in vibration problems. This is why in recent years it has become a powerful tool for modal analysis.

Considering the ideas above, this work seeks to analyse the normal modes of vibration of the body components of a C-Bandola: how they interact, how they are coupled and how they change to conform to the instrument. The analysis is performed using the finite element method (FEM), a known numerical method with wide applications. This study will complement previous work done on the acoustic analysis of this instrument, which since early 2010 has been developed under the courses Advanced Project I-II of the Engineering Physics program of the Universidad EAFIT. This thesis is intended not only to contribute to academia, but also, to impact the future in bandola's musical performance: an useful tool could be provided to national luthiers in order to supply some information about the instrument response and possibly propose modifications to control sound parameters.

1.4   State of the Art

Previous analysis of the bandola's acoustic properties

The acoustic study of Colombian Andine Bandola was proposed in early 2010 and began within the courses Advanced Project I-II of the Engineering Physics program. The projects developed in those courses were *Planteamiento de una metodología de medida acústica en la bandola andina colombiana* (Approach to an acoustic measurement methodology in the Colombian Andean Bandola) and *Caracterización acústica de la afinación y los modos normales de vibración en bandolas colombianas* (Acoustic characterization of pitch and the normal modes of vibration in Colombian bandolas), whose results led to the establishment of a measurement methodology for the characterization of tuning and the visualization of normal modes of vibration by interferometric optical techniques [2, 3]. The review of measurement techniques and the foundations in the acoustic field were the introduction to a wide discipline which is not very common in the national panorama. The development of the projects was intended to measurements that could be achieved with available resources and thus, without specialized devices and/or spaces designed specifically for related purposes. However, this study prompted the integration of different fields such as optics which facilitated the analysis.

As a complement to experimental studies that were fulfilled, the proposal for a numerical approach to study the modal characteristics of the instrument was suggested.

Related works

The modal analysis as a technique for studying dynamic properties of structures began to be developed experimentally in the 1960s, which David L. Brown and Randall J. Allemang [4] called "The modern era of experimental modal analysis". This is due to the confluence of several technologies that were developed earlier in the century and became integrated in the 1960s. Furthermore, the theoretical support of this technique was formulated and developed from the 1930s to 1950s and already well-established in the literature of 1963. Thus, it can be said clearly that the onset of this new era was framed in the mid-60s, when the theory was already developed and the hardware, in terms of sensors and measuring equipment, was commercially available.

Although musical acoustics is supported by two treatises of the late nineteenth century, "Tonempfindungen" of Helmholtz and "Theory of Sound" of Rayleigh, the beginning of greater research and bibliographic production initiate in 1960s with authors

such as A. Benade, C. Hutchins and J. C. Schelleng [5]. The latter two authors begin in this decade with the study of the acoustics of the violin and by the end of it, the study of the guitar is promoted. In the early 1970s the use of modal analysis techniques on these instruments was then conducive. At this point, the modal problem in the resonance box of the instruments –its resonances and the modal coupling present in dynamic behavior– began to be treated in more detail, analytically and experimentally.

Authors such as M. Firth, Meyer, O. Christensen, B. Vistisen, G. Caldersmith, R. Boullosa, T. Dickens, V. Jansson, D. Rossing, among others, present studies on these aspects of vibrational behavior in guitars and violins [6–27]. For example on the issue of modal coupling, the work of Meyer, Fletcher and Rossing [11,18] recognize the three lowest modal frequencies of the classical guitar body as combination modes; the top and back plates and the enclosed air in the cavity vibrate as one body, thereby producing these first three resonances. Other studies about the frequencies of top plate modes were carried out during this period by Jansson [15], Boullosa [20], Christensen [7] and Rossing [12].

With the advent of great computational advances and because of the inconvenient fact that many of the issues addressed had no analytical solution, a new approach began to be considered. Numerical analysis in musical acoustics was first seen in the mid-80s and specifically the Finite Element Methods (FEM) received great acceptance in the modal analysis of musical instruments [33]. Considering that experimental implementation of modal analysis was quite expensive, FEM became a powerful computational tool to predict the modal behavior of structures. It is noteworthy that in the early 1960s there was already sufficient literature on the investigation of the FEM numerical technique [34], so at the time of its use in musical acoustics, the technique was sufficiently developed.

There are representative sources in numerical analysis of string instruments (especially guitars) that leads one to distinguish two types of analysis: transient (time-domain) and stationary analysis. On these two issues the work of Elejabarrieta, Derveaux, Bécache, among others [35–54], have established a representative source of reference for the first decade of the 21st century.

Considering the development of modal analysis in musical instruments, especially the numerical development, the study of modal coupling in a Colombian Andine Bandola in C using the Finite Element Method is proposed. Similar results to those of the guitar are expected because the building and physical conditions are nearly the same, except for the geometry.

Chapter 2

Theoretical Framework

2.1   The Colombian Andean Bandola

In order to get familiar with the structure and operating mechanism of the musical instrument of analysis, this section introduces Colombian Andean C-Bandola and its main structural characteristics.

Colombian Andean Bandola is a plucked string instrument that comes from guitar family. Its name comes from an old persian-arabic root, pandur, that comes through different north african and european instruments and indicates a variety of melodic instruments with high and medium pitch. This instrument presents several design adaptations through history in different Colombian regions that differ essentially in dimensions, process of building and tuning. Bandola in C (tuned in C) and bandola in B♭ (tuned in B♭) are the most representative prototypes.

The analysis proposed in this document is considered for bandola in C, which has been accepted and markedly used in last years by *estudiantinas* (musical groups similar to Tunas). Hence, following descriptions pertain to this instrument with C-tuning.

Bandola in C, specially found in Bogotá savanna, presents twelve strings grouped in unison pairs. Strings form six groups tuned in intervals of perfect fourths [1]. Figure 2.1 presents the bandola and the pitchs for each string. The frequency values that correspond to the tuning of each open string are specified in Table 2.1.

Constitutive parts of bandola are shown in Figure 2.2. Definition of parts and their structural function can be found in [1].

According to Figure 2.2, substructures are formed by grouping listed parts. This is:
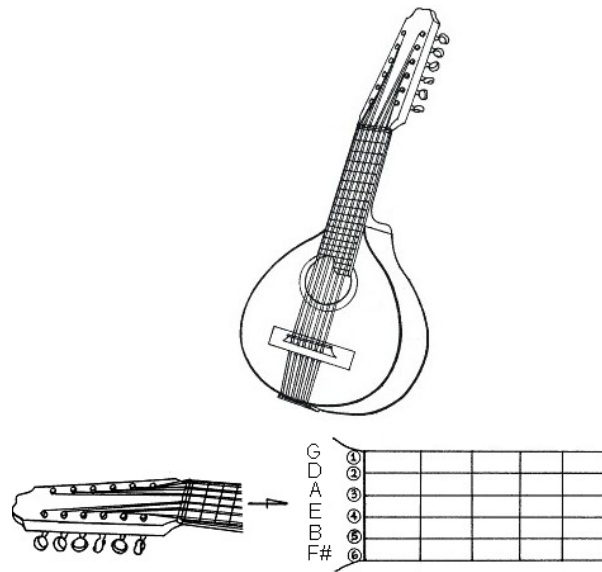
Figure 2.1: Upper image: Colombian Andean Bandola. Lower image: Pitch for each string. From top to bottom in fingerboard strings are tuned in: G, D, A, E, B, F♯

Frequencies of tuning for the open strings					
	G4	D4	A3	E3	B2	F♯ 2
Hz	783.99	587.33	440	329.63	246.94	185

Table 2.1: Frequency values that correspond to the tuning of open strings in the Bandola

- Mast: Formed by

  1. Headstock

  2. Handle or neck

  3. Heel

  4. *Zoque* or Heel brick.

- Resonance box: Formed by

  5. Back plate

  6. Reinforcement bars

  7. Upper brick

17
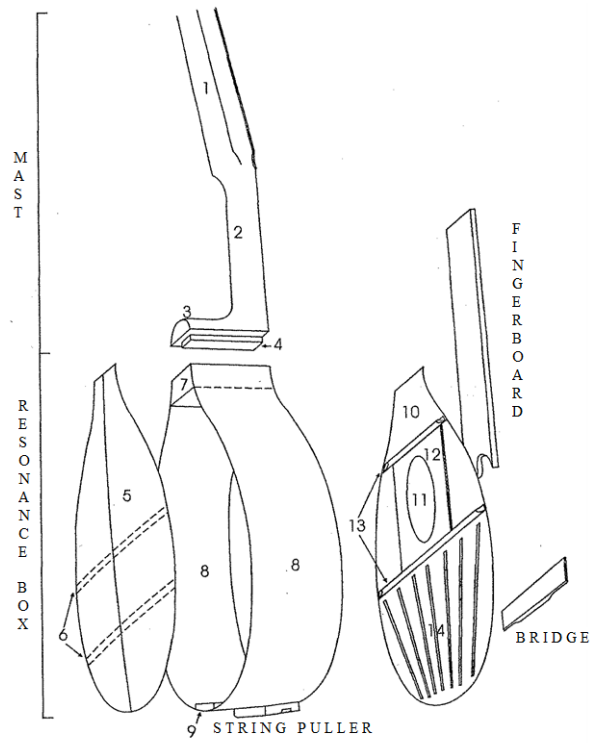
Figure 2.2: Bandola's constitutive parts

   8. Ribs

   9. Lower brick

  10. Top plate

  11. Soundhole

  12. Soundhole reinforcement

  13. Harmonic bars

  14. Fan bracing

- Nut

- Fingerboard

- Bridge

- String puller

2.2 Musical Acoustics and Stringed Musical Instruments closer to the Bandola

Musical Acoustics is a branch of acoustics which studies how is produced, propagated and perceived the sound with musical proposes. This concept immediately relates the idea of physics in musical instruments, i.e., how wind, brass or any type of musical instrument physically works [55].

Sources of sound in instruments could be of mechanical, acoustical or electrical type. For instance, vibrations of strings, bars, membranes, plates, air in a tube and synthesized sounds. Even sources could be collective coupled vibrators, in other words, a complex system [11]. Related to this fact, instrument analysis is classified according the type of source or sound production. This will indicate the phenomenon involved in each case, and thus, the useful mathematical formulation useful.

String instruments are a particular case of classification, which commonly, not only involve string vibration in an instrument, but also coupled plates, bars and air oscillations. Violins, guitars and bandola in C are examples in this category and many works have been devoted, at least for violins and guitars, to study their behavior as complex system [6–11].

For simplicity, complex systems are divided in subsystems. Thus, the phenomena involved in guitars sound production will be presented, as an exponent, by distinguishing two main subsystems: the first composed by strings, bridge and top plate and the second composed by guitar body parts. Due to the great similarity of guitar and bandola, this example constitutes an excellent description to illustrate physical behavior of bandola in C.

In Figure 2.3, a scheme similar to one presented in [11] shows the frequency range in which each subsystem play significant role. From this figure, guitar behavior can be described as follows: At low frequency, guitar transmits vibrations through the bridge to the top plate, which displaces fluid inside the cavity and induces pressure changes that cause soundhole radiation. Vibrational energy is also transmitted to back plate via both the ribs and air cavity pressure changes. At high frequency, most of the sound is radiated by top plate and the role of the bridge becomes more relevant.

A detailed individual subsystem behavior could be described, but such specific task
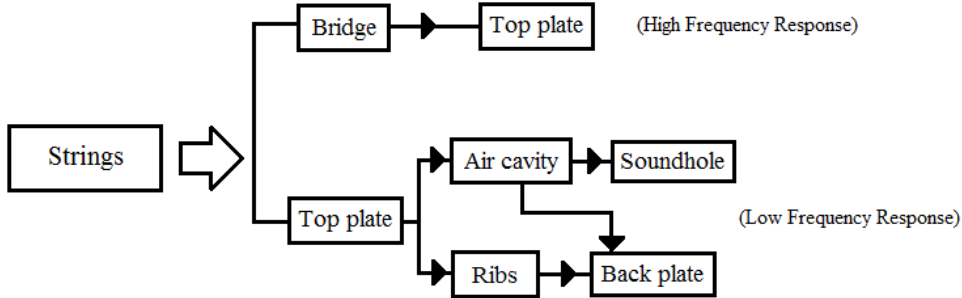
Figure 2.3: Scheme of guitar subsystems according to frequency response

is not of interest in this document except for the analysis of modal coupling at low resonances in instrument body. This subject will be developed throughout the document. For more detail, the document bibliography covers different related topics and [11] presents a good summary of them.

2.3 Wood: Considerations for musical instruments

Wood is an elastic anisotropic material which elastic behavior depends on observation scale. The effective properties of this material depends on the length scale of the excitation, i.e., the response is not the same for different length scales [56]. For wavelengths bigger than microstructural dimensions, the anisotropy is assumed to have elastic symmetry in three planes that are perpendicular to each other (taking in mind tree growing). This anisotropy is called orthotropy and is characterized by nine independent constants in stiffness tensor. Figure 2.4 shows trees orthotropy.

As Figure 2.4 shows, independent mechanical properties contained in the stiffness tensor, are oriented in the three mutually perpendicular axes: longitudinal L, tangential T and radial R. The mechanical properties of interest are:

- Young's modulus: A measure of stiffness of an elastic material, i.e., the ratio of uniaxial stress σ_i over uniaxial strain ε_i for elastic deformations. Thus, Young's Modulus in the *ith* direction is defined:

$$E_i = \frac{\sigma_i}{\varepsilon_i} \quad \text{where } i = 1, 2, 3$$
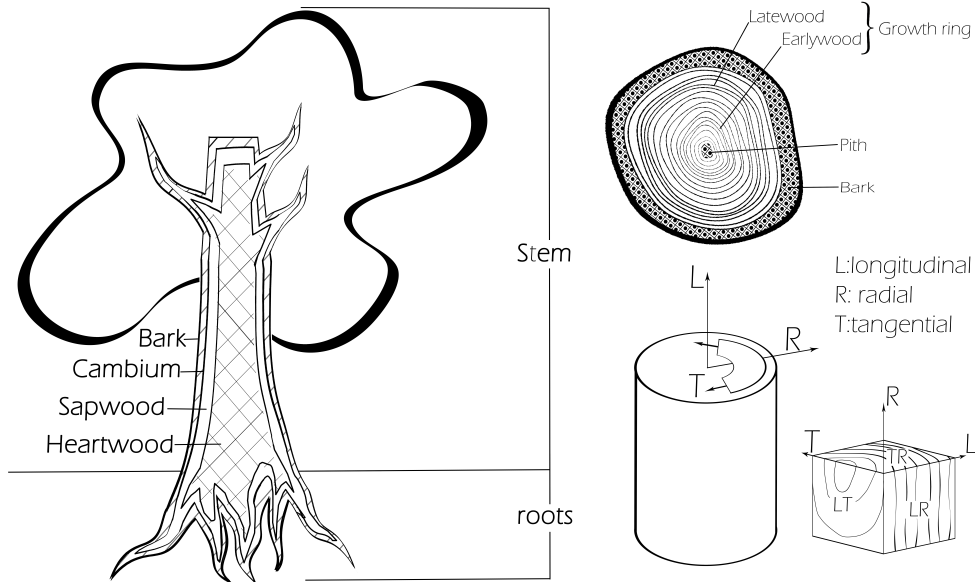
Figure 2.4: Trees orthotropy. Due to tree growth, wood structure can be described using the three mutually perpendicular axes: longitudinal L, tangential T and radial R

- Poisson's ratio: Ratio of transverse strain ε_j in *jth* direction, over axial strain ε_i in *ith* direction when axial stress is applied. Thus,

$$\nu_{ij} = -\frac{\varepsilon_j}{\varepsilon_i}$$

- Shear modulus: Ratio of shear stress σ_{ij} over the shear strain ε_{ij}. Thus, Shear Modulus in ij planes is defined:

$$G_{ij} = -\frac{\sigma_{ij}}{\varepsilon_{ij}}$$

Luthiers have established the most appropriate wood species and cuts for musical instruments. For instance, spruce is generally admitted for guitars top plate under the term *resonance wood*; curly maple for back plate, ribs, and neck again is a resonance wood [56].

A resonance wood has remarkably regular anatomical structure. Thus, a narrow grain spruce is preferred for guitars although cedar is also used. Curly maple has

a aesthetic criterion of selection, but for guitar back and sides, hardwoods of high densities and low damping are used.

As mentioned, also wood cuts represent an important parameter in order to control acoustic properties of wood. There are three possible wood cuts to use for string instrument parts as Figure 2.5 shows, i.e., Quarter sawn, rift sawn and flat sawn.
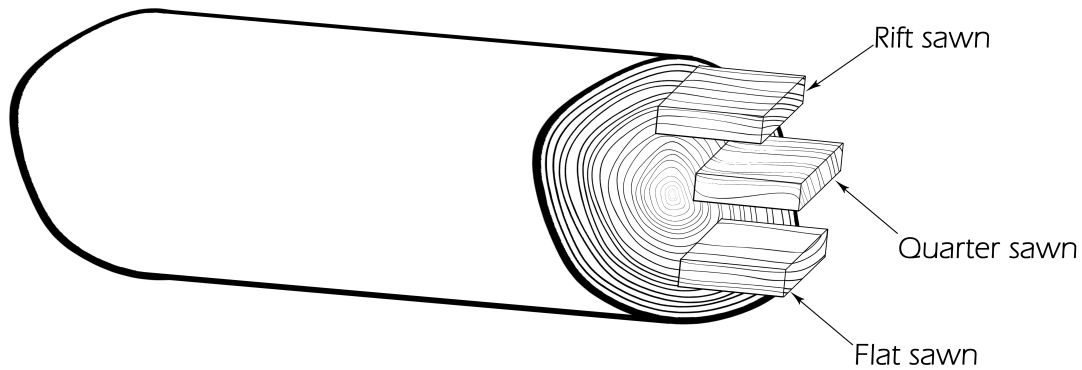
Figure 2.5: Possible wood cuts for string instrument building

Wood is considered quarter sawn when its growth rings are 60 to 90 degrees to the face of the board. Rift sawn wood is where the growth rings are between 45 and 60 degrees to the face of the board. Flat sawn wood has its growth rings 30 degrees or less with the face.

Quarter swan presents the most regular anatomical structure, thus, this cut is ideal for top plates. Figure 2.6 presents an stem with several possible quarter sawn.

Even with these presented wood complex considerations for musical instruments, there is another important feature that has to be considered in order to build a good instrument: moisture. Instrument stiffness depends on wood moisture and hence, the restoring forces determined by elastic properties also depend on it.

A young wood would have high moisture that yields poor stiffness. Old woods with poor moisture are excessively rigid. Thus, only a balanced moisture in wood that means a mature wood, is suitable for musical instruments.
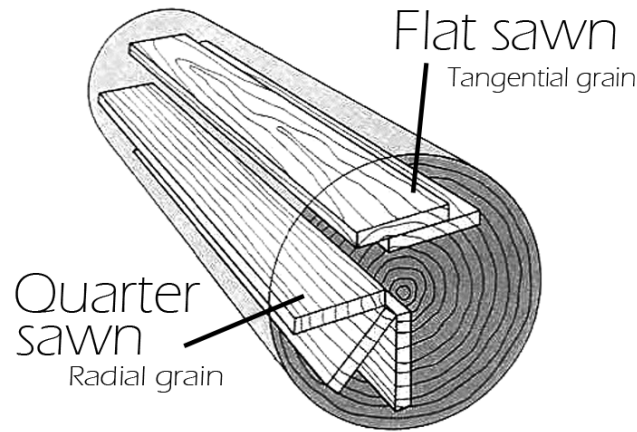
Figure 2.6: Stem with quarter swan

2.4 Structural Dynamics: Theory of Plates

The study of structures behavior has been important specially for aeronautical, civil and mechanical engineering and many efforts have been made in order to develop theories that describes how beams, shells and plates work, as integral parts of structures. With a wide range of applications, plate theory is an old topic that has been assisted by numerical procedures and has become an useful tool to analyse in detail simple or complex dynamic problems.

This section contains the main aspects of classical plate theory for transverse vibrations which is valid for low modes. This theory neglects transverse shear effects as well as rotatory inertia effect that are important when the plate is relatively thick or when higher-mode vibration characteristics are needed [57].

Thus, classical plate theory or Kirchhoff plate theory is based on the following assumptions:

1. Thickness of the plate is small when compared with other dimensions.

2. Normal stresses in the direction transverse to the plate are taken to be negligibly small.

3. Effect of rotatory inertia is negligible.

4. Normal to the undeformed middle surface remains straight and normal to the deformed middle surface and unstretched in length.

These assumptions are illustrated in Figure.2.7
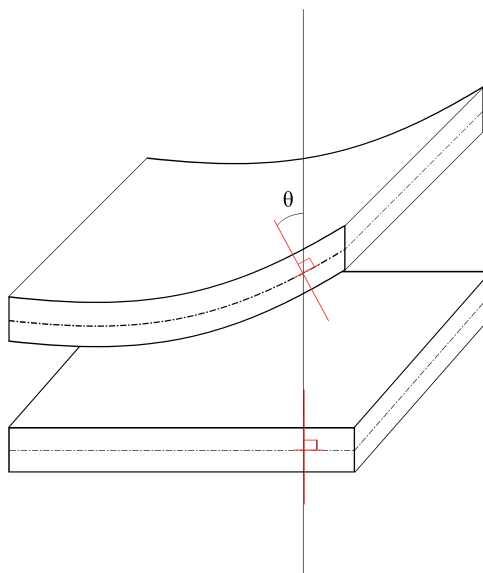
Figure 2.7: Deformation in a Kirchhoff plate.

Plate equations for Isotropic and Orthotropic (with a plane of isotropy) material are introduced now.

2.4.1   Isotropic plates

Using generalized Hooke's law in in Voigt notation [58] to relates stresses and strains of an isotropic material yields

$$
\begin{Bmatrix} \sigma_1 \\ \sigma_2 \\ \sigma_3 \\ \sigma_{23} \\ \sigma_{31} \\ \sigma_{12} \end{Bmatrix} = \begin{bmatrix} c_{11} & c_{12} & c_{12} & 0 & 0 & 0 \\ c_{12} & c_{11} & c_{12} & 0 & 0 & 0 \\ c_{12} & c_{12} & c_{11} & 0 & 0 & 0 \\ 0 & 0 & 0 & (c_{11}-c_{12})/2 & 0 & 0 \\ 0 & 0 & 0 & 0 & (c_{11}-c_{12})/2 & 0 \\ 0 & 0 & 0 & 0 & 0 & (c_{11}-c_{12})/2 \end{bmatrix} \begin{Bmatrix} \varepsilon_1 \\ \varepsilon_2 \\ \varepsilon_3 \\ \varepsilon_{23} \\ \varepsilon_{31} \\ \varepsilon_{12} \end{Bmatrix}. \quad (2.1)
$$

24

Here σ_i and ε_i are stresses and strains in ith direction (where $i = 1, 2, 3$) in a plane with normal in the ith direction; σ_{ij} and ε_{ij} are the shear stresses and shear strains perpendicular to i axis and parallel to j axis; and c_{ij} is an element of the stiffness matrix C. For isotropic materials there are only two independent constants in C as it can be observed in Eq.2.1, i.e., c_{11} and c_{12}. Stiffness matrix C contains common engineering constants that include Young's Modulus E_i, Poisson's ratio ν_{ij} and the shear modulus G_{ij}. Assuming a lamina in a plane 1-2 (say xy plane) and thus, a plane stress defined by $\sigma_z = 0$, $\sigma_{yz} = 0$, σ_{zx}, i.e., $\sigma_3 = 0$, $\sigma_{23} = 0$, $\sigma_{31} = 0$; the stress-strain relation in terms of stiffness matrix is

$$\begin{Bmatrix} \sigma_1 \\ \sigma_2 \\ \sigma_{12} \end{Bmatrix} = \begin{bmatrix} \frac{E}{1-\nu^2} & \frac{\nu E}{1-\nu^2} & 0 \\ \frac{\nu E}{1-\nu^2} & \frac{E}{1-\nu^2} & 0 \\ 0 & 0 & \frac{E}{2(1+\nu)} \end{bmatrix} \begin{Bmatrix} \varepsilon_1 \\ \varepsilon_2 \\ \varepsilon_{12} \end{Bmatrix},$$

where $E_1 = E_2 = E_3 = E$, $G_{23} = G_{31} = G_{12} = E/2(1+\nu)$ and $\nu_{23} = \nu_{31} = \nu_{12} = \nu$.

Isotropy allows considerable simplification in dynamic plate equation for transverse vibrations. The procedure to obtain the equation can be followed in references [57] and [59]. Thus, the dynamic equation of plates yields

$$D\nabla^4 w + \rho h \frac{\partial^2 w}{\partial t^2} = 0 \tag{2.2}$$

where w is the plate transverse displacement; ρ is the density of the plate material; h is the plate thickness; D is the flexural rigidity; and ∇^4 the biharmonic operator. D and ∇^4 (in Cartesian coordinates) are defined as follows:

$$D = \frac{Eh^3}{12(1-\nu^2)}$$
$$\nabla^4 w = \frac{\partial^4 w}{\partial x^4} + 2\frac{\partial^4 w}{\partial x^2 \partial y^2} + \frac{\partial^4 w}{\partial y^4}$$

For thin plate theory, boundary conditions which are parallel to the x-direction are

$$\text{either } w = 0 \quad \text{or} \quad V_y = 0$$
$$\text{either } \frac{\partial w}{\partial y} = 0 \quad \text{or} \quad M_y = 0;$$

and those parallel to y-direction are

$$\text{either } w = 0 \quad \text{or} \quad V_x = 0$$
$$\text{either } \frac{\partial w}{\partial x} = 0 \quad \text{or} \quad M_x = 0.$$

Here, M_x and M_y are bending moments in x and y directions; V_x and V_y are combinations of transverse shear force and the rate change of bending moment in direction tangent to the edge. They are defined as

$$
\begin{aligned}
M_x &= -D\left[\frac{\partial^2 w}{\partial x^2} + \nu\frac{\partial^2 w}{\partial y^2}\right] \\
M_y &= -D\left[\frac{\partial^2 w}{\partial y^2} + \nu\frac{\partial^2 w}{\partial x^2}\right] \\
V_x &= -D\left[\frac{\partial^3 w}{\partial x^3} + (2-\nu)\frac{\partial^3 w}{\partial x\partial y^2}\right] \\
V_y &= -D\left[\frac{\partial^3 w}{\partial y^3} + (2-\nu)\frac{\partial^3 w}{\partial x^2\partial y}\right]
\end{aligned}
$$

For instance, possible combinations (physically consistent) of boundary conditions along an edge in x-direction are:

- Clamped edge: $w = \frac{\partial w}{\partial y} = 0$.

- Simply supported or fixed edge: $w = M_y = 0$.

- Free edge: $M_y = V_y = 0$

Going back to Eq.2.2, the solution $w(x, y, t)$ for free vibrations can be expressed as

$$w(x, y, t) = W(x, y)e^{i\omega t}. \tag{2.3}$$

By substituting Eq.2.3 in Eq.2.2 yields

$$(\nabla^4 - \beta^4)W(x, y) = 0,$$

where $\beta^4 = \rho h\omega/D$.

Differential operator can be factored into

$$(\nabla^2 + \beta^2)(\nabla^2 - \beta^2)W = 0,$$

whose solution is a sum of solutions that arise from

$$
\begin{aligned}
(\nabla^2 + \beta^2)W_1 &= 0 \\
(\nabla^2 - \beta^2)W_2 &= 0.
\end{aligned}
$$

Thus, the original solution of Eq.2.2 must have the form

$$W = W_1 + W_2.$$

2.4.2   Orthotropic plates with a plane of isotropy

As isotropic plates, generalized Hooke's law of an orthotropic material under plane stress can be expressed in terms of engineering constants. Thus,

$$\left\{ \begin{array}{c} \sigma_1 \\ \sigma_2 \\ \sigma_{12} \end{array} \right\} = \left[\begin{array}{ccc} \frac{E_1}{1-\nu_{12}\nu_{21}} & \frac{\nu_{12}E_2}{1-\nu_{12}\nu_{21}} & 0 \\ \frac{\nu_{21}E_1}{1-\nu_{12}\nu_{21}} & \frac{E_2}{1-\nu_{12}\nu_{21}} & 0 \\ 0 & 0 & 2G_{12} \end{array} \right] \left\{ \begin{array}{c} \varepsilon_1 \\ \varepsilon_2 \\ \varepsilon_{12} \end{array} \right\},$$

where

$$\frac{\nu_{12}}{E_1} = \frac{\nu_{21}}{E_2}$$

With four independent variables, this relation generalize the $D\nabla^4 w$ term in Eq.2.2 and yields,

$$D_1 \frac{\partial^4 w}{\partial x^4} + D_2 \frac{\partial^4 w}{\partial x^2 \partial y^2} + D_3 \frac{\partial^4 w}{\partial y^4}$$

Variational methods are a different way to deal the problem in order to find a solution to this new equation. These methods find functions that minimize or maximize the value of a quantity. In this way, orthotropic plate vibration is approximated trough strain energy functional (the quantity) which is commonly minimized. Thus, the strain energy functional for an orthotropic laminated plate is

$$U_s = \frac{1}{2} \int_A \left[D_{11} \left(\frac{\partial^2 w_0}{x^2} \right)^2 + D_{22} \left(\frac{\partial^2 w_0}{\partial y^2} \right)^2 + 4D_{66} \left(\frac{\partial^2 w_0}{\partial x \partial y} \right)^2 + 2D_{12} \left(\frac{\partial^2 w_0}{\partial x^2} \right) \left(\frac{\partial^2 w_0}{\partial y^2} \right) \right] dA$$

where U_s is the strain energy, A the outer boundary and

$$
\begin{aligned}
D_{11} &= \frac{E_1 h^3}{12(1 - \nu_{12}\nu_{21})} \\
D_{22} &= \frac{E_2 h^3}{12(1 - \nu_{21}\nu_{12})} \\
D_{12} &= D_1 \nu_{21} \\
D_{66} &= \frac{G_{12} h^3}{12}
\end{aligned}
$$

2.5   Acoustic Waves

An acoustic wave is a particular example of pressure fluctuation in compressible fluid. This type of wave describes the phenomenon for inviscid fluids with small amplitude of vibration, small amount of density variation and small fluid velocity (that neglects convective effects).

For inviscid fluids, wave propagation occurs when the fluid is compressed or expanded and produces pressure changes that act as restoring forces. Individual fluid elements oscillates about an equilibrium position and generate regions of compression and rarefaction that propagate a longitudinal wave.

Linear *Euler*'s equation is valid to describe dynamic fluid behavior about the hydrostatic state in processes of small amplitude, this is

$$\rho_0 \frac{\partial v}{\partial t} = -\nabla p, \tag{2.4}$$

where v is fluid velocity; ρ_0 is the fluid density in the hydrostatic state; and p the pressure. This expression also considers ρ_0 as a constant, neglects convective effects and viscous effect.

Using continuity equation for fluids

$$\rho_0 \nabla \cdot v = -\frac{\partial \rho}{\partial t}$$

where

$$\frac{\partial \rho}{\partial t} \approx \frac{\rho_0}{K_s} \frac{\partial p}{\partial t},$$

by taking its time derivative, yields

$$\rho_0 \nabla \cdot \left(\frac{\partial v}{\partial t} \right) = \frac{\rho_0}{K} \frac{\partial^2 p}{\partial t^2}, \tag{2.5}$$

where K_s the bulk modulus. If it is applied divergence in Eq.2.4

$$\rho_0 \nabla \cdot \left(\frac{\partial v}{\partial t} \right) = -\nabla \cdot (\nabla p) \tag{2.6}$$

where $\nabla \cdot (\nabla p) = \nabla^2 p$, substituting Eq.2.5 in Eq.2.6 yields

$$\nabla^2 p = \frac{1}{c^2} \frac{\partial^2 p}{\partial t^2} \tag{2.7}$$

where the speed of sound is defined by

$$c = \sqrt{\frac{K_s}{\rho_0}}. \qquad (2.8)$$

Expression in Eq.2.7 is the known acoustic wave equation.

2.6 Fluid-Structure Coupling

While studying physical behavior of systems, one can find frequently a system linked to others (one or more) where its description depends on the simultaneous description of the others. Therefore, an independent solution is impossible without the parallel solutions of the rest. Such systems are called coupled and the way they interact will determine the coupled system behavior.

Examples of coupled systems are those which involve (not always) different physical phenomena, i.e., thermal-structural, thermal-electromagnetic, electrostatic-structural and fluid-structural couplings to mention a few. This section describes a known formulation of a fluid-structure coupling that concerns us for understanding the problem proposed in this document.

Dynamic fluid-structure interaction can be followed when the motion of the structure induces pressure changes on the fluid (which doesn't penetrate the structure) and produces fluctuating motions. As the fluid moves, the varying pressure field loads the structure and its motion is modified. Thus, the process starts again.

Since dynamical considerations of linear motion are made on each system: fluid and structure, it will be developed the case of small vibrations while interaction is substantial. Moreover, it is assumed the particular case of interaction via a domain interface[1]. It is worthwhile to clear that a static case doesn't imply the coupling and it is the dynamic problem that is found to be coupled.

With this background and considering dynamic equations for structures and fluids presented in the last two section, it will be expressed the equations for a fluid structure coupling through Galerkin's variational method ("The weak form") which is useful in finite element method formulation. Once the weak form of coupled system is reached, the discrete form will be presented.

---

[1]Many works have been devoted to this interaction when the fluid is contained, which is of considerable engineering interest. A good reference in the subject of coupled systems is [60]

2.6.1 Weak form of Coupled system

The Helmholtz equation for acoustic problems in Eq.2.7

$$\nabla^2 p = \frac{1}{c^2}\frac{\partial^2 p}{\partial t^2},$$

can be expressed according to variational method as

$$\delta\Pi_f = \int_{\Omega_f} \delta p \left[\frac{1}{c^2}\frac{\partial^2 p}{\partial t^2} - \nabla^2 p\right]d\Omega = 0.$$

After integrations by parts using Green's first identity yields

$$\int_{\Omega_f}\left[\delta p \frac{1}{c^2}\frac{\partial^2 p}{\partial t^2} + (\nabla\delta p)^T(\nabla p)\right]d\Omega + \int_{\Gamma}\delta p(\nabla p \cdot n)d\Gamma = 0,$$

where Ω_f is the fluid domain and Γ is the boundary part where boundary conditions must be specified. Since the fluid is coupled with the motion of the structure, thus, the condition here is:

$$\dot{v}_n = \ddot{u}_n = \mathbf{n^T}\ddot{\mathbf{u}}. \tag{2.9}$$

where $\mathbf{n}$ is the direction cosine vector for an outward pointing normal to the fluid region and $\dot{v}$ is prescribed.

Using E.q.2.4, this boundary condition yields

$$\int_{\Omega_f}\left[\delta p\frac{1}{c^2}\frac{\partial^2 p}{\partial t^2} + (\nabla\delta p)^T(\nabla p)\right]d\Omega + \int_{\Gamma_1}\delta p\rho_0\mathbf{n^T}\ddot{\mathbf{u}}d\Gamma = 0, \tag{2.10}$$

Also, the weak form for solids can be presented as

$$\int_{\Omega}\delta\mathbf{u^T}(\rho_s\ddot{\mathbf{u}} + \mu\dot{\mathbf{u}} + \mathbf{S^T DSu} - \mathbf{b})d\Omega - \int_{\Gamma_t}\delta\mathbf{u^T}\bar{\mathbf{t}}d\Gamma = 0, \tag{2.11}$$

where ρ_s is the density of the solid, μ a damping constant, $\mathbf{S}$ a linear differential operator, $\mathbf{D}$ the elasticity matrix containing the material properties and $\bar{\mathbf{t}}$ is the surface traction defined as

$$\bar{\mathbf{t}} = -p\mathbf{n_s} = p\mathbf{n}.$$

Above equation takes a positive pressure in compression and the outward normal to the solid $n_s = -n$. The traction integral in Eq. 2.11 is now expressed as

$$\int_{\Gamma_t} \delta \mathbf{u^T} \bar{\mathbf{t}} d\Gamma = \int_{\Gamma_t} \delta \mathbf{u^T} \mathbf{n} p d\Gamma.$$

It can be observed that both weak forms for fluid and solid depend on a variable defined in the other coupled phenomenon. This indicates the mutual dependence, i.e., the coupling.

2.6.2   Discretized coupled system

In Eq.2.10 and Eq.2.11, pressure and displacement vectors p and u will be approximated to discretize the system. For this, a shape function is proposed in order to fix pressure and displacement values in a specific domain. This can be expressed as

$$\begin{aligned} p &\approx \hat{p} = N_p \tilde{p} \\ u &\approx \hat{u} = N_u \tilde{u} \end{aligned}$$

where $\tilde{p}$ and $\tilde{u}$ are the values for pressure and displacement at every point defined in the domain and N_p and N_u are appropriate shape functions that fix the values at the points in the domain.

Thus, discretization applied to fluid equation in Eq.2.10 yields

$$S\ddot{\tilde{p}} + H\tilde{p} + \rho_0 Q^T \ddot{\tilde{u}} + q = 0, \tag{2.12}$$

where q is an included source term and

$$\left. \begin{aligned} S &= \int_\Omega N_p^T \frac{1}{c^2} N_p d\Omega \\ H &= \int_\Omega (\nabla N_p)^T \nabla N_p d\Omega \\ Q &= \int_{\Gamma_t} N_u^T \mathbf{n} N_p d\Gamma \end{aligned} \right\} \tag{2.13}$$

Similarly, the discrete structural problem becomes

$$M\ddot{\tilde{u}} + C\dot{\tilde{u}} + K\tilde{u} - Q\tilde{p} + f = 0, \tag{2.14}$$

where

$$
\begin{aligned}
M &= \int_\Omega N_u^T \rho_s N_u d\Omega \\
C &= \int_\Omega N_u^T \mu N_u d\Omega \\
K &= \int_\Omega B^T D B d\Omega \\
q &= -\int_\Omega N_u b d\Omega.
\end{aligned}
$$

$B = SN_u$ and Q is identical to Eq. 2.13.

If free vibrations are considered and all forces and damping terms are omitted, Eq.2.12 and Eq.2.14 can be written as

$$
\begin{bmatrix} M & 0 \\ \rho_0 Q^T & S \end{bmatrix} \begin{Bmatrix} \ddot{\tilde{u}} \\ \ddot{\tilde{p}} \end{Bmatrix} + \begin{bmatrix} K & -Q \\ 0 & H \end{bmatrix} \begin{Bmatrix} \tilde{u} \\ \tilde{p} \end{Bmatrix} = 0
$$

For an eigenvalue problem, it is observed immediately that the system is not symmetric nor positive definite and standard eigenvalue extraction methods are not direct applicable. However, it is physically clear that eigenvalues are real and free vibration modes exist.

In [60] is presented a simple method to achieve symmetrization introducing a new variable $\tilde{p} = \omega^2 \tilde{q}$. This yields in the generalized eigenvalue problem:

$$
\left(\begin{bmatrix} K & 0 & 0 \\ 0 & \frac{1}{\rho_0} S & 0 \\ 0 & 0 & 0 \end{bmatrix} - \omega^2 \begin{bmatrix} M & 0 & Q \\ 0 & 0 & \frac{1}{\rho_0} S \\ Q^T & \frac{1}{\rho_0} S^T & -\frac{1}{\rho_0} H \end{bmatrix} \right) \begin{Bmatrix} \tilde{u} \\ \tilde{p} \\ \tilde{q} \end{Bmatrix} = 0
$$

2.7 Modal Analysis

Most of practical noise and vibration problems are related to resonance phenomenon: forces applied to a system excite one or more modes of vibration and they, as a discrete set, define the forced or free response. Modal analysis studies dynamic properties in an elastic structure via the identification of modes of vibration. This field describes

dynamic response of a system through the modal parameters: resonance natural frequencies, damping factor and mode shape vectors. These parameters constitute a complete dynamic description of the structure and thus, elastic behavior could be predicted, corrected or even "controlled" if they are known [62].

It is very important to clear that free and forced vibrations are two successive stages in a full vibration analysis. A free vibration analysis yields the information about modal parameters using mechanical properties, whereas a particular type of forced analysis leads to the definition of a frequency response function such as mobility, the ratio of velocity response to force input [61].

Measure and analysis of structure dynamic response, when excited by an input, can be done by simultaneously collecting the input and output signals in time domain. Such signals are transformed to frequency domain and the ratio of input spectrum over the output spectrum yields the system function. The inverse of this system function is defined as the transfer function or Frequency Response Function (FRF), which contains the information about system dynamic properties independently of signal input type (either harmonic, transitory or random excitations).

The general structural problem is

$$M\ddot{u} + C\dot{u} + Ku = f \tag{2.15}$$

where M, C and K are mass, damping and stiffness matrices respectively; u and f are displacement and applied force vectors. By applying Laplace transform in Eq.2.15 yields

$$B(s)X(s) = F(s), \tag{2.16}$$

where

$$B(s) = Ms^2 + Cs + K; \tag{2.17}$$

and s is the Laplace variable.

$B(s)$ is the system function and thus, $H(s) = B(s)^{-1}$, is the FRF. Eq.2.16 could be written as

$$X(s) = H(s)F(s)$$

After these basic considerations of modal analysis, it is worthwhile to clear what normal modes mean. A normal mode of vibration is an inherent movement configuration of a structure which is determined by geometry, material properties and boundary conditions characteristics. In a normal mode, every point of the structure moves at the same frequency with a fixed relative phase, i.e., all points reach their maximum

or minimum displacement at the same time. Figure 2.8 shows five normal modes of vibration of a classical guitar top plate reported in [15].
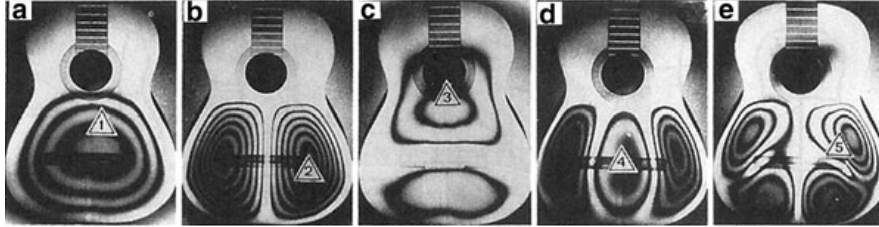

Figure 2.8: Vibration modes (with holographic interferometry) of a classical guitar top plate glued to fixed ribs but without the back [15].

In order to find normal modes in a structure, the eigenvalue problem is solved for system matrix $B(s)$ where the roots of polynomial in Eq. 2.17 are the eigenvalues or poles as it will be shown.

If the elements of system matrix $B(s)$ are quadratic functions of s, transfer function $H(s)$ and its elements h_{ij} can be written as follows

$$
\begin{aligned}
H(s) &= \frac{1}{det(B(s))} adj(B(s)) \\
h_{ij} &= \frac{g(s)}{det(B(s))}
\end{aligned}
$$

where $det(B(s))$ is the known characteristic polynomial and the values when $det(B(s)) = 0$ are the poles of transfer function. Physically, the poles are the frequency values in which the structure presents the lowest resistance to vibrate. This values make transfer function go to infinite, and this is interpreted as a state of resonance of the system.

Each pole pair is said to be a mode of vibration, this is expressed as follows

$$
p_k = \xi_k \pm i\omega_k
$$

where

$$
\begin{aligned}
p_k &= \text{system modal pole} \\
\xi_k &= \text{damping modal coefficient} \\
\omega_k &= \text{the damped angular frequency.}
\end{aligned}
$$

Thus, the resonance angular frequency is given by

$$\Omega_k = \sqrt{\xi_k^2 + \omega_k^2}$$

and the damping ratio

$$\zeta = \frac{\xi_k}{\Omega_k}.$$

When $\zeta_k = 1$, mode k is critically damped, when $\zeta_k < 1$, mode k is under-damped and when $\zeta_k > 1$, mode k is over-damped. When the system is under-damped, poles are complex and occur in conjugated pairs; when the system is critically damped or over-damped, poles are real values and are along the real axis in the complex domain of s.

It is worthwhile to mention that for under-damped situation, the system will oscillate at the natural damped frequency ω_k, which is a function of the natural frequency ω_n and the damping ratio. Thus,

$$\omega_k = \omega_n \sqrt{1 - \zeta^2}$$

Modal vectors u_k are defined as solutions of the following homogeneous equation

$$B(p_k)u_k = 0,$$

where u_k is a complex vector. Considering this, transfer matrix is written as a sum of complex pairs

$$H(s) = \sum_{k=1}^{n} \left[\frac{u_k u_k^T}{s - p_k} + \frac{u_k^* u_k^{*T}}{s - p_k^*} \right]$$

where $*$ denotes complex conjugate and T denotes transposed. Each term in the sum is a $n \times n$ matrix that represents the contribution of mode k in transfer function. Modal vectors and pole localization can be identified from any row or column of transfer matrix, except for those corresponding to zero modal vectors (nodal points). This fact makes possible the most significant conclusions in modal analysis.

2.8   Finite Element Method

Finite Element Method (FEM) is a numerical technique suitable for analysis of complex structures with irregular geometries. This technique has many applications for

engineering processes, specially when behavior prediction is needed but experimental analysis implies high costs compared with benefits.

FEM is used as an approximation to continuum problems. The continuum is divided in finite sub-domains called elements and the solution of the problem is given by the elements assembly. The problems treated are boundary value problems and it is possible to define them as standard discrete systems [60]. Figure 2.9 shows the generic discrete structural problem defined for an element from a discretized domain, where M is the element mass matrix, C is the element damping matrix, K is the element stiffness matrix and F is the load vector over the element.
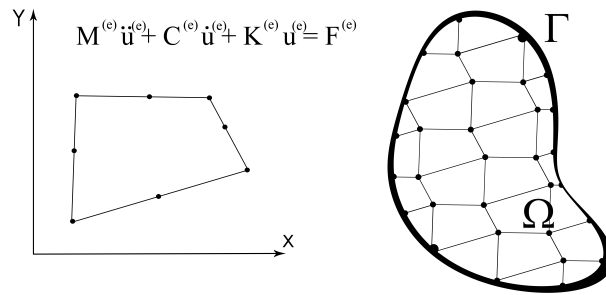

Figure 2.9: Element from a discrete domain in which generic discrete structural equation is defined

Boundary value problems are defined by differential equations that depend on the analysed phenomenon. Although some problems have exact analytical solutions that may be identified, for others a closed solution doesn't exist and different methods are used to approximate them. Variational methods are used with this purpose and as mentioned before, they find functions to minimize or maximize system quantities. Particularly, Galerkin's method uses a variational principle and converts the differential operator problem to a integral operator problem (weak formulation), which finally takes the form of a discrete one via an interpolation method [63]. This can be illustrated as follows.

The general form of a partial differential equation (PDE) with two independent variables $u = u(x, y)$ defined over a bi-dimensional domain Ω, is

$$a\frac{\partial^2 u}{\partial x^2} + 2h\frac{\partial^2 u}{\partial x \partial y} + b\frac{\partial^2 u}{\partial y^2} + f = 0,$$

where a, b and h are real constants or functions of x and y, and f is a function of $\partial u/\partial x$, $\partial u/\partial y$ and u.

Using variational principle, it is defined a quantity $\Pi(v)$ called functional which is minimized when $\Pi(u)$, being u the solution of the problem. Here, v is an arbitrary function in the same domain of u where

$$v \in L^2 = \left\{ v : \Omega \longrightarrow \Re \quad \text{such that} \quad \int_\Omega v^2 d\Omega < \infty \right\}$$

and L^2 is the space of square-integrable functions.

Thus, variational method transform PDE into a integration problem as follows:

$$\Pi = \int_\Omega \left(a\frac{\partial^2 u}{\partial x^2} + 2h\frac{\partial^2 u}{\partial x \partial y} + b\frac{\partial^2 u}{\partial y^2} \right) v d\Omega + \int_\Omega f v d\Omega = 0. \qquad (2.18)$$

After integration by parts, commonly trough Green's first identity, Eq.2.18 takes the *weak form*.

Galerkin's method consist of defining u and v as functions of the same space of functions V, where $V \in L^2$. Considering $\{N_1, N_2, ...\}$ as a base that spans the space V, then, it can be expressed:

$$u(x, y) = \sum_i \alpha_i N_i(x, y).$$

Function u can be approximated by a base of finite dimension as

$$u(x, y) \cong \hat{u} = \sum_i^n \tilde{u}_i N_i(x, y),$$

where u_i is the value of the function at a point (x_i, y_i). Similarly for $v(x, y)$

$$v(x, y) \cong \hat{v} = \sum_i^n \tilde{v}_i N_i(x, y).$$

These approximations of u and v yields each, a system of equations that can be

expressed as a standard discrete system, i.e., a matrix-vector form $\mathbf{N}\tilde{\mathbf{u}} = \hat{u}$:

$$
\begin{bmatrix} N_1 & N_2 & N_3 & \cdots \end{bmatrix} \begin{Bmatrix} \tilde{u}_1 \\ \tilde{u}_2 \\ \tilde{u}_3 \\ \vdots \end{Bmatrix} = \hat{u} \tag{2.19}
$$

$$
\begin{bmatrix} N_1 & N_2 & N_3 & \cdots \end{bmatrix} \begin{Bmatrix} \tilde{v}_1 \\ \tilde{v}_2 \\ \tilde{v}_3 \\ \vdots \end{Bmatrix} = \hat{v} \tag{2.20}
$$

Given a specific PDE and its functional, Eq.2.19 and Eq.2.20 can be used and thus obtain a discrete system as in Eq.2.12 and Eq.2.14.

This solution approximation is made at every sub-domain or element where shape functions $\mathbf{N}(\mathbf{x}, \mathbf{y})$ fix solution values at some points (nodes) defined in the element. Global solution could be found in element assembly, forming a global matrix-vector expression.

Chapter 3

Methodology

According to the stated specific objectives, the methodology of analysis can be followed throughout two stages. The first one defines the numerical model considerations that were made in order to tackle the problem and the second one presents developed CAD models and simulation procedure for analysis.

The mentioned stages contain the following main topics:

- **Model considerations.**

  1. It defines two coupling models that describe each dynamic behavior of bandola at it first two and three resonance frequencies.
  2. It defines some characteristics of the elements [1] considered for coupling models, i.e, material characteristics and boundary conditions.

- **CAD models and simulation procedure.**

  1. It presents CAD models of elements considered in couplings models.
  2. It presents the main characteristics of modal analysis by FEM of uncoupled elements.
  3. It presents the main characteristics of modal analysis by FEM of coupled elements in each coupling model.

---

[1]It is worthwhile to consider that throughout the document the word *Element* will be used in two situations. It may refer to elements or oscillators of coupling models and also, to elements that form the mesh in the Finite Element Method.

Methodology of analysis can be resumed in the scheme of Figure 3.1.
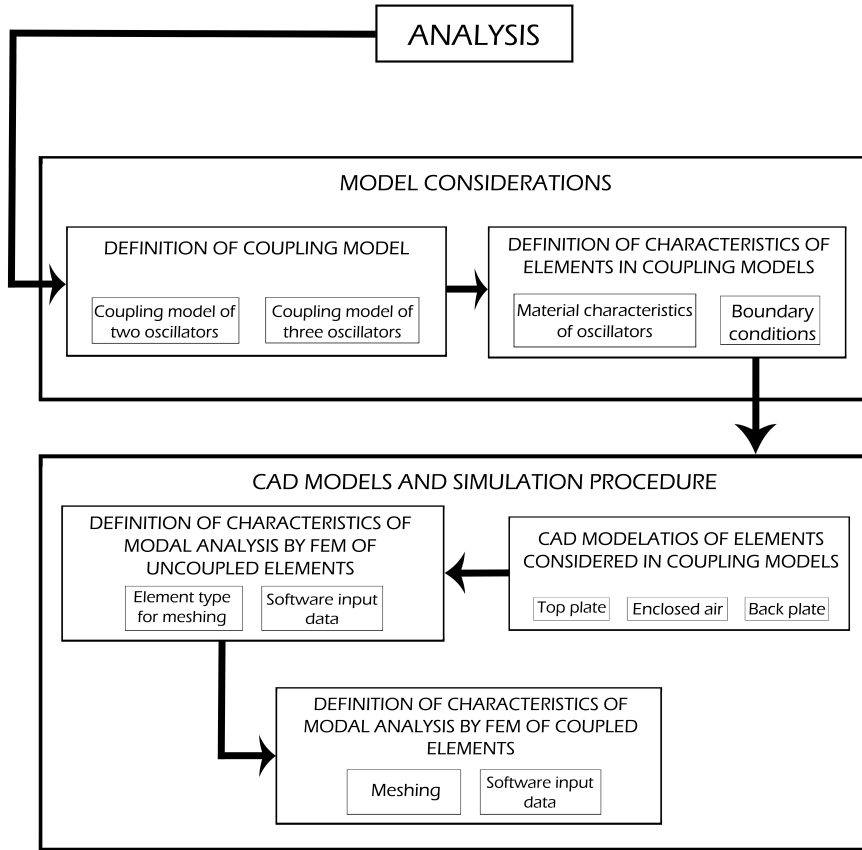
Figure 3.1: Scheme that outlines the methodology of analysis.

3.1 Numerical model considerations.

In order to convert the physical problem to a mathematical model, certain assumptions are made to define differential equations governing the mathematical model. The finite element analysis solves this mathematical model, and all assumptions in it will be reflected in the predicted response: It cannot be expected more information in the prediction of physical phenomena than the information contained in the mathematical

model [34]. Hence, it is very important to define an appropriate mathematical model (and thus, the numerical model) for the analysis purposes stated in this document.

Numerical models are approximations of physical phenomena and are built through mathematical models. These approximations or simplifications allow a gradual approach to the problem since more realistic working model can be established at later stages. In musical acoustics, for example, McIntyre and Woodhouse [24] expose the importance of divide the complex physical system of musical instruments into simpler components and thus, these may be studied and modelled in simpler interactions. For stringed instruments they identify three systems: the strings, the body and the radiation of sound, but they also point out that these systems cannot be entirely separated because there are important interactions between them.

Modal coupling analysis at low resonances in a bandola can be performed by assuming a coupling model for resonance box. Reported works on the subject [6–13, 18, 19] analyse commonly two coupling models, each with two and three coupled oscillators respectively. For instance, Meyer, Rossing and Christensen [8, 12, 18] describe that three coupled oscillators: top plate, enclosed air and back plate, produce the first three modal frequencies of a classical guitar resonance box which correspond to combination modes. Considering works in [7, 13, 19], these authors also reported that a model with two oscillators: top plate and enclosed air, will predict the first two resonances.

According to above ideas and taking in mind that guitars are the closest acoustical reference of bandolas, numerical models that reflect these coupled systems are proposed for modal coupling analysis. Thus, numerical solutions could describe dynamic behavior in the bandola at its first two or three resonances for each case. The scheme in Figure 3.2 presents the conditions that should be evaluated and included in a numerical model for simulating modal coupling at low frequencies in a Colombian Andean Bandola. These conditions refer mainly to: constitutive elements of coupling, their material features and boundary conditions.

At this point, model considerations are specified throughout two subsections. First subsection, "coupled systems", presents coupling models by describing an illustrative case of coupled vibrating systems that allow understanding useful characteristics of coupled oscillators. Then, it will be described both the coupled system of top plate and enclosed air and the coupled system of top plate, enclosed air and back plate. This way of introduction of coupling model allows to contrast between the two type of coupled systems, being more general the one that considers three oscillators.

Finally, in second subsection: "Individual parts considerations", are evaluated and
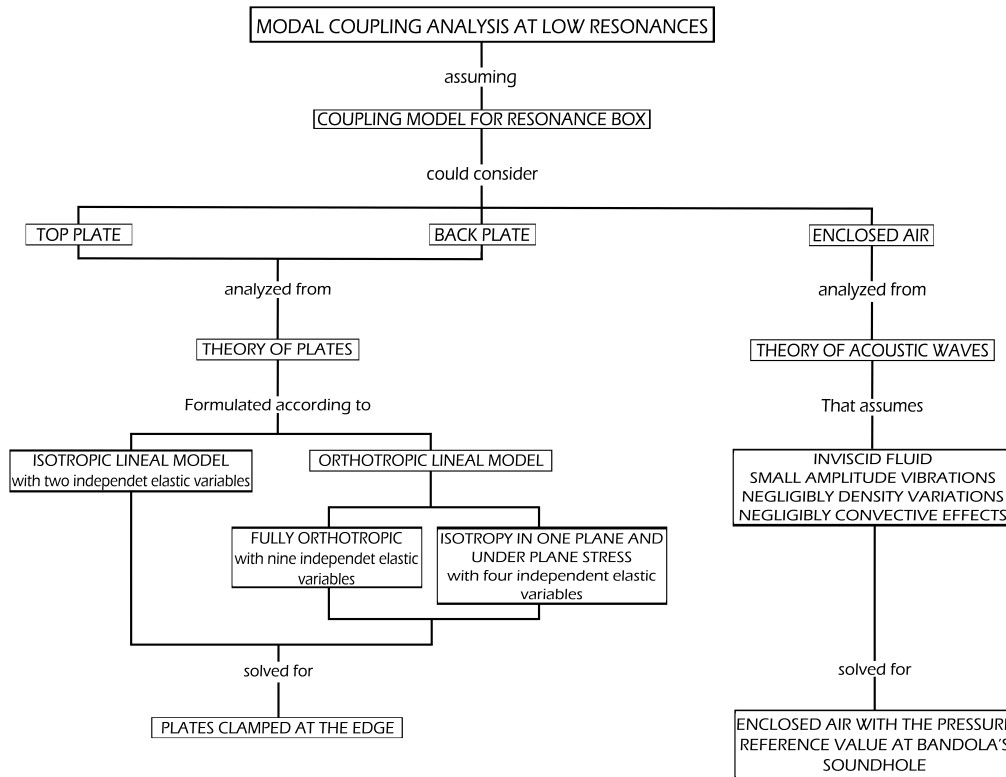
Figure 3.2: Scheme that outlines the way in which problem is tackled: Dynamic behavior is studied through modal coupling at low resonances between bandola's plates and enclosed air. Different dynamic expressions, that will be coupled eventually, describe behavior of plates and enclosed air and state necessary conditions for problem solution.

defined the material characteristics and boundary conditions of each element or oscillator according to phenomenon conditions. The numerical solution of models will depend on these considerations.

3.1.1 Coupled systems.

Normal modes of a two-mass system.

Further understanding of coupling phenomenon could be achieved by considering the two-mass system in Figure 3.3. Such a system, as it will shown, could be viewed as two

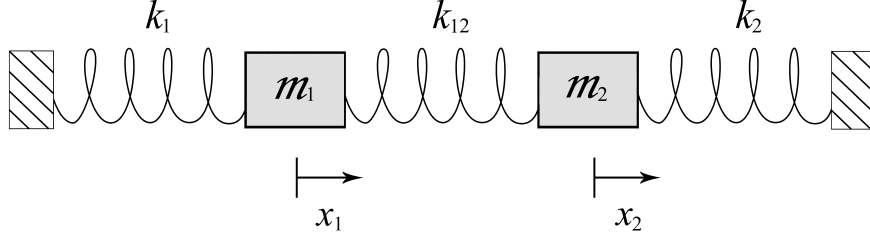separate mass/spring vibrators coupled together by the center spring.

Figure 3.3: Oscillating system consisting of two masses and three springs.

From Figure 3.3 it can be expressed:

$$- m_1\ddot{x}_1 = k_1 x_1 + k_{12} x_1 - k_{12} x_2 \tag{3.1}$$
$$-m_2\ddot{x}_2 = k_2 x_2 + k_{12} x_2 - k_{12} x_1 \tag{3.2}$$

Assuming harmonic solutions $x_j = A_j e^{i\omega t}$ with $j = 1, 2$ and using matrix-vector form, then:

$$\begin{bmatrix} k_{12} + k_1 & -k_{12} \\ -k_{12} & k_{12} + k_2 \end{bmatrix} \begin{Bmatrix} x_1 \\ x_2 \end{Bmatrix} - \omega^2 \begin{bmatrix} m_1 & 0 \\ 0 & m_2 \end{bmatrix} \begin{Bmatrix} x_1 \\ x_2 \end{Bmatrix} = 0 \tag{3.3}$$

Considering $k_1 = k_2 = k$ and grouping the expression, the solution of the system is found by making characteristic polynomial equal to zero:

$$\det(K - \omega^2 M) = 0 \tag{3.4}$$

$$\left(\frac{k_{12} + k}{m_1} - \omega^2 \right) \left(\frac{k_{12} + k}{m_2} - \omega^2 \right) - \frac{k_{12}^2}{m_1 m_2} = 0, \tag{3.5}$$

where M is the mass matrix and K is the stiffness matrix. Thus,

$$\omega_1^2 = \left[\left[(k_{12}^2 + 2kk_{12} + k^2)m_2^2 + (2k_{12}^2 - 4kk_{12} - 2k^2)m1m2 + (k_{12}^2 + 2kk_{12} + k^2)m_1^2 \right]^{1/2} \right.$$
$$\left. + (k_{12} + k)m_2 + (k_{12} + k)m_1 \right] / (2m_1 m_2) \tag{3.6}$$

$$\omega_2^2 = - \left[\left[(k_{12}^2 + 2kk_{12} + k^2)m_2^2 + (2k_{12}^2 - 4kk_{12} - 2k^2)m1m2 + (k_{12}^2 + 2kk_{12} + k^2)m_1^2 \right]^{1/2} \right.$$
$$\left. + (-k_{12} - k)m_2 + (-k_{12} - k)m_1 \right] / (2m_1 m_2) \tag{3.7}$$

The importance of these expressions comes out with the next relation:

$$\omega_1^2 + \omega_2^2 = \frac{k}{m_1} + \frac{k}{m_2} + \frac{k_{12}}{m_1} + \frac{k_{12}}{m_2}.$$

For separate mass/spring systems $\omega_{01}^2 = k/m_1$ and $\omega_{02}^2 = k/m_2$. With $\omega_c^2 = k_{12}/m_1 + k_{12}/m_2$, it can be expressed:

$$\omega_1^2 + \omega_2^2 = \omega_{01}^2 + \omega_{02}^2 + \omega_c^2 \tag{3.8}$$

This relation in Eq.3.8 contains an important concept: resulting coupled resonance frequencies can be expressed as a combination of uncoupled resonance frequencies of individual oscillators and a coupling term ω_c^2.

The value of resonance frequencies as functions of spring stiffness also leads to an important idea. By taking the limits for Eq.3.6 and Eq.3.7 in which k_{12} tends to zero and to infinity, yields:

$$\lim_{k_{12} \to 0} \omega_1^2 = \omega_{01}^2 \tag{3.9}$$

$$\lim_{k_{12} \to 0} \omega_2^2 = \omega_{02}^2 \tag{3.10}$$

$$\lim_{k_{12} \to \infty} \omega_1^2 = \infty \tag{3.11}$$

$$\lim_{k_{12} \to \infty} \omega_2^2 = \frac{2k}{m_2 + m_1} \tag{3.12}$$

Assuming a particular case for E.q3.6 and E.q.3.7 where $m_1 = 1$, $m_2 = 2$ and $k = 1$, it can be plotted resonance frequencies as functions of spring stiffness. Figure 3.4 and Figure 3.5 show the plots for each resonance frequency.

It is observed in Figure 3.4 that ω_1^2 is plotted as function of $\tan(k_{12})$ in order to represent the bound when k_{12} tends to infinity.

The limits when spring stiffness k_{12} tends to zero implies separate oscillations since oscillators are no longer coupled. Thus, each separate system vibrates at its single resonance frequency, ω_1^2 and ω_2^2 respectively. Moreover, limits when spring stiffness k_{12} tends to infinity don't converge necessarily and it is only defined a bound for ω_2^2. This bound represent a rigid body movement since the spring is completely rigid and fixes the two masses.

The descriptions that have been made about two-mass coupled system lead to propose modal analysis for each oscillator of the coupling models that concern us. Obtaining resonance frequencies of each oscillator and their mode shapes, will allow to
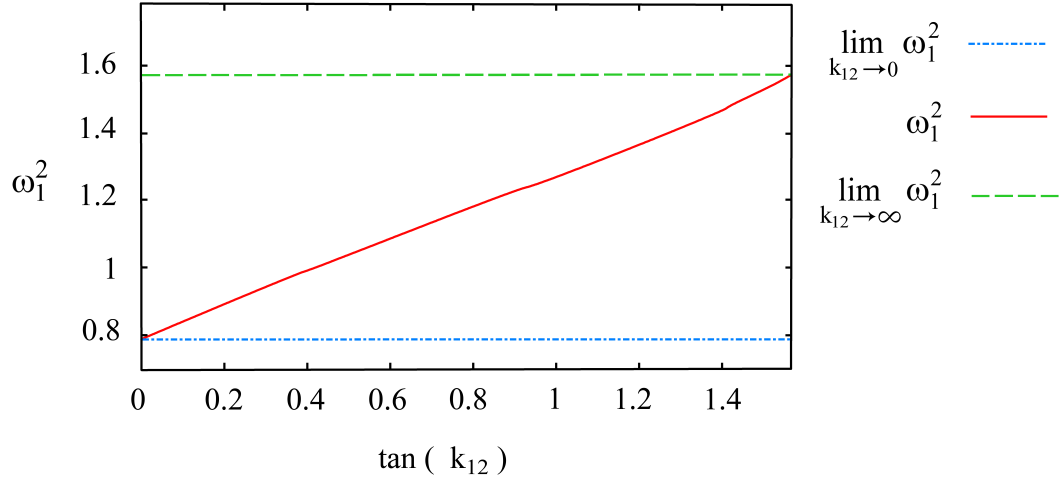
Figure 3.4: First resonance frequency Vs magnitude of k_{12}.

compare and correlate qualitatively the modes of coupled and uncoupled resonances and also to verify relation in Eq.3.8.

Coupling between top plate and enclosed air.

Vibrations of the top plate produce small periodic variations of cavity volume which change the air pressure inside the cavity. This process forces the air in and out through the sound hole as an air piston driven by a restoring force, which is provided by air pressure changes inside the cavity. Air pressure on top plate surface feeds the motion of the plate and couples the system.

Based on the model presented by Christensen and Vistisen in [7], the coupling between top plate and enclosed air is presented on the basis of Newtonian equations of motion. The model consider the interaction of resonances of two oscillators: Helmholtz resonance and the fundamental top plate resonance. The air inside the cavity vibrates somehow like a Helmholtz resonator for the first mode. In this case, this resonator consist of an air piston in the sound hole, oscillating against the stiffness of the air in the cavity. The fundamental top plate mode in a guitar is characterized by symmetrical variation of amplitude over the lower bout of the guitar [15], hence, the model consider this fundamental resonance assuming a simple harmonic oscillator consisting of a plate mass and a piston area, together with a spring stiffness. The back plate is assumed
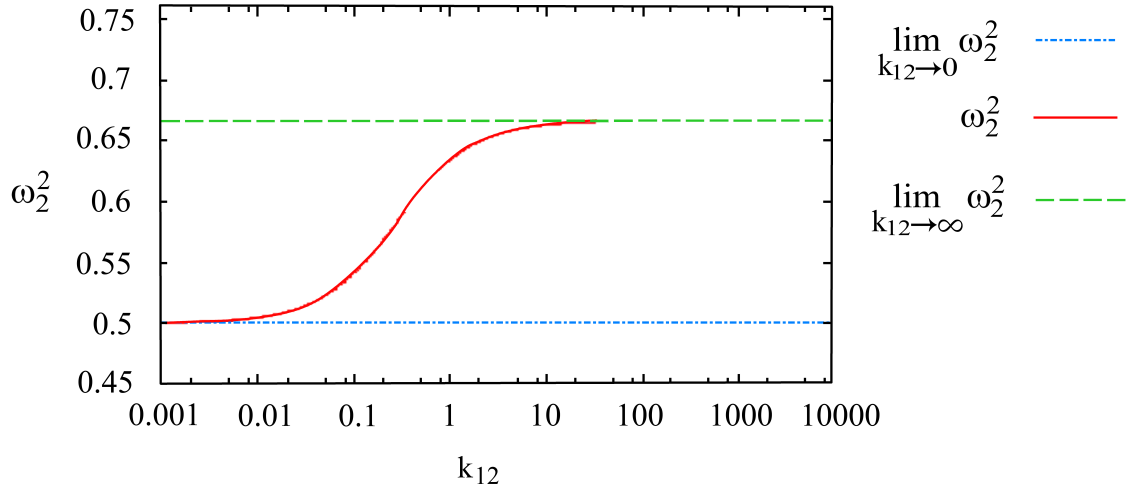
Figure 3.5: Second resonance frequency Vs magnitude of k_{12}.

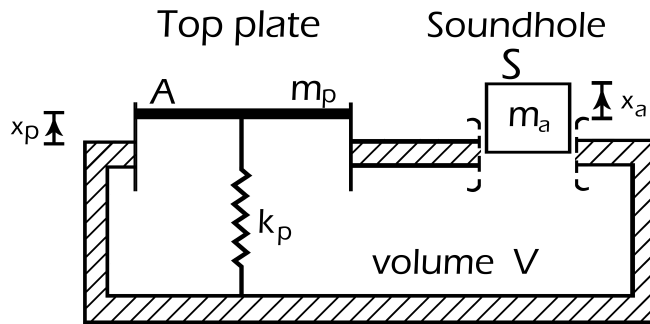rigid. Figure 3.6 illustrates the model.

Figure 3.6: Coupling model of resonance box of two oscillators presented by Christensen and Vistisen

Equations of motion for the system of two coupled oscillators are:

$$m_p \ddot{x}_p = -k_p x_p + A \Delta p \qquad (3.13)$$
$$m_a \ddot{x}_a = S \Delta p, \qquad (3.14)$$

where $\Delta p = -\mu \Delta V$, $\mu = c^2 \rho_a / V$, $\Delta V = A x_p + S x_a$ and

$$
\begin{aligned}
x_p & \quad \text{the displacement of top plate piston} \\
x_a & \quad \text{the displacement of air piston} \\
m_p & \quad \text{the plate mass} \\
m_a & \quad \text{the air piston mass} \\
k_p & \quad \text{the spring stiffness} \\
A & \quad \text{the equivalent piston area of top plate} \\
S & \quad \text{the area of soundhole} \\
c & \quad \text{the sound velocity in air} \\
\rho_a & \quad \text{the density of air} \\
V & \quad \text{the cavity volume}
\end{aligned}
$$

As presented in the example for a two-mass system, assuming $x_p = A_p e^{i\omega_p t}$ and $x_a = A_a e^{i\omega_h t}$ in E.q.3.13 and E.q.3.14 and using a matrix-vector form, solution of the system is found for the characteristic polynomial:

$$
(\omega^2 - \frac{k_p + \mu A^2}{m_p})(\omega^2 - \frac{\mu S^2}{m_a}) - \frac{(\mu S A)^2}{m_p m_a} = 0. \tag{3.15}
$$

It can be noted from E.q.3.13 and E.q.3.14 that resonance frequencies for both separate systems (plate and piston air) ω_p and ω_h respectively, are:

$$
\omega_p^2 = \frac{k_p + \mu A^2}{m_p}
$$

$$
\omega_h^2 = \frac{\mu S^2}{m_a}
$$

With $\omega_{ph}^4 = (\mu S A)^2 / m_p m_a$ as a coupling frequency, E.q.3.15 yields:

$$
(\omega^2 - \omega_p^2)(\omega^2 - \omega_h^2) - \omega_{ph}^4 = 0, \tag{3.16}
$$

and its roots or resonances frequencies can be expressed as:

$$
\omega_{1,2}^2 = \frac{1}{2}(\omega_p^2 + \omega_h^2) \pm \frac{1}{2}\sqrt{(\omega_p^2 - \omega_h^2)^2 + 4\omega_{ph}^4}. \tag{3.17}
$$

For this system of two oscillators, an important relation can be given by summing both roots in E.q.3.17:

$$\omega_1^2 + \omega_2^2 = \omega_p^2 + \omega_h^2 \tag{3.18}$$

Above equation says that square sum of the resonance frequencies in the coupled system equals the square sum of resonances frequencies in the uncoupled system. An expression very similar to that presented in E.q.3.8.

The model presented by Christensen and Vistinsen is validated through mobility and sound radiation measurements that confirm the great approach to guitar dynamic behavior at the first two resonances. As they mentioned [7], "the only condition for establishment of a coupling is that the Helmholtz resonance is present and that the vibration of the top plate (plus back plate eventually) generates a net volume displacement". Therefore, the behavior of bandola at the first two resonances is assumed to be described by this model, and the use of FEM will give a wider scope since it considers an extended body which allows detailed information at every point.

Coupling between top plate, enclosed air and back plate.

The influence of the back plate is modelled by introducing another piston with effective area B and mass m_b which acts against a spring of stiffness k_b, as described by Christensen [8]. Motion of any piston causes pressure changes inside the cavity and will affect the motion of the other two pistons. The the system of coupled pistons is given in Figure 3.7.
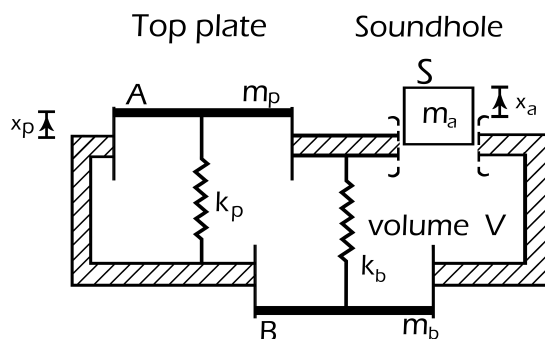

Figure 3.7: Coupling model of resonance box of three oscillators presented by Christensen

The equations of motion for the three pistons in the coupled system are:

$$m_p\ddot{x}_p = -k_p x_p + A\Delta p \tag{3.19}$$

$$m_a\ddot{x}_a = S\Delta p \tag{3.20}$$

$$m_b\ddot{x}_b = -k_b x_b + B\Delta p, \tag{3.21}$$

where x_b is the displacement of back plate piston. Δp, as before, is the pressure change in the cavity resulting from movements of the pistons. Thus,

$$\Delta p = -\mu\Delta V$$
$$\Delta V = Ax_p + Sx_a + Bx_b$$

Again, it is assumed $x_p = A_p e^{i\omega_p t}$, $x_a = A_a e^{i\omega_h t}$ and $x_b = A_b e^{i\omega_b t}$ for equations in Eqs.3.19-3.21. Thus, it can be identified that:

$$
\begin{aligned}
\omega_p^2 &= \frac{k_p + \mu A^2}{m_p} & \omega_{phh}^2 &= \frac{\mu S A^2}{m_a} & \omega_{hbb}^2 &= \frac{\mu S B^2}{m_b} \\
\omega_h^2 &= \frac{\mu S^2}{m_a} & \omega_{php}^2 &= \frac{\mu S A^2}{m_p} & \omega_{pbp}^2 &= \frac{\mu A B^2}{m_p} \\
\omega_h^2 &= \frac{k_b + \mu B^2}{m_b} & \omega_{hbh}^2 &= \frac{\mu S B^2}{m_a} & \omega_{pbb}^2 &= \frac{\mu A B^2}{m_b}
\end{aligned}
\tag{3.22}
$$

Using the matrix-vector form, characteristic polynomial yields:

$$\omega_{pbp}^2\omega_{phh}^2\omega_{hbb}^2 + \omega_{hbh}^2\omega_{php}^2\omega_{pbb}^2 - \omega_{pbp}^2\omega_{pbb}^2\omega_h^2 - \omega_{hbh}^2\omega_{hbb}^2\omega_p^2 - \omega_b^2\omega_{php}^2\omega_{phh}^2 + \omega_p^2\omega_h^2\omega_b^2 = 0.$$

Roots of this polynomial are large expression that won't be presented, but instead is shown, by summing the roots, that it is also held the relation where the square sum of coupled resonance frequencies is equal to the sum of uncoupled resonance frequencies. Thus,

$$\omega_1^2 + \omega_2^2 + \omega_3^2 = \omega_p^2 + \omega_h^2 + \omega_b^2 \tag{3.23}$$

Meyer [19] was the first one to give a detailed technical description for the three-oscillators system. He showed that the effect of back plate is to lower ω_1 and ω_2 and to split ω_2 in two resonances yielding ω_3.

This model is used for description of bandola behavior at the first three resonances, where again the use of FEM will give a wider scope. It was observed that coupled modes are expressed in terms of uncoupled modes, so, numerical models for separate

oscillators (of each model) are proposed for analysis in order to appreciate, through comparison, their participation in coupled modes.

An useful detail for analysis can be noted in coupling frequency terms. These terms are ratios of the piston areas and the effective mass of oscillating pistons, with more terms for the case of three oscillators as shown in Eq.3.22. It can be infer of this fact that a weak or strong coupling will depend on this ratios.

A qualitatively comparison between both models presented (models of two and three oscillators) can be made. Basically, the use of these two coupling models will be useful as reference for numerical models and also for numerical results which must reflect predictions of coupling models and will provide further understanding since extended bodies can be modelled.

3.1.2 Individual parts considerations.

Material properties.

It is an important aspect to state the material properties into the numerical models. Although models of coupled systems presented above don't have any specification of material properties, stiffness terms in models contain the information of *effective* material properties. For instance, elastic behavior of plates material determines the relation between the applied forces and resultant displacements (Hooke's law), thus, the way in which oscillators will vibrate depends on its elastic features that, in fact, define how rigid or how much resistance to movement the material presents.

Numerical models for the analysis are built on the basis of presented coupling models, consequently, mathematical models used in FEM, wich are formulated from theories of plates and acoustic waves, reflect the coupled systems. Material properties are specified in dynamic equations of plates and acoustic waves (as it was presented in the theoretical framework) and in the case of plates, the formulation of equations will vary according to an isotropic or orthotropic material.

Acoustic waves are assumed to propagate in an inviscid fluid with small amplitudes of vibration, negligibly density variations and negligibly convective effects. Wave propagation will thus depend only on fluid density ρ_a and its bulk modulus K_s. For air, using relation in 2.8, the values can be specified as follows:

$$\begin{aligned} \rho_a &= 1.18 kg/m^3 \\ c &= 343 m/s \end{aligned}$$

Moreover, Bandola's plates are made of wood, an orthotropic material which according to the way it was extracted from the tree, could present transverse isotropy. For plates of musical instruments transverse isotropy is common and their material properties are thus specified through five elastic values: E_x, E_y, ν_{xy}, G_{xy} and ρ_p. Although orthotropic properties can be introduced in numerical models, dynamic expressions for plates could be simplified by considering isotropic properties which also simplify numerical computing.

The modal analysis proposed in this work is dedicated to study the coupling phenomenon at low resonances, and simple numerical models are pursued in order to ease monitoring the influence of some specific model parameters. The effect of orthotropy over coupling won't be considered as analysis subject, therefore, plates material will be modelled as an isotropic material.

For isotropy, elastic values of *Young's Modulus* and *Poisson's ratio* are defined through the geometric mean of properties presented for spruce in [25] and rosewood in [27]. Using a numerical model of the bandola's top plate, different methods were tested for finding appropriate values for elastic properties. Modal analysis was performed with ANSYS® for both an orthotropic and isotropic plates; isotropic values were averaged by arithmetic mean, geometric mean and a method which minimized the square Frobenius norm of the difference between each constitutive tensor of orthotropic and isotropic material. Comparing first three resonance frequencies of both orthotropic and isotropic models, geometric mean approached the values that had an effect close to orthotropy, i.e., frequency values similar to those of orthotropic plate.

The elastic properties in [25] and [27] that were used for the average are presented in Table 3.1. Wood densities are also presented in this table. The averaged values for isotropic plates are presented in Table 3.2.

Material with transverse isotropy					
	ρ_p (kg/m^3)	E_x (GPa)	E_y (GPa)	ν_{xy}	G_{xy} (GPa)
Top plate (Spruce)	330	0.66	6.6	0.003	0.77
Back Plate (Rosewood)	775	2.2	16	0.05	1.1

Table 3.1: Elastic properties for material with transverse isotropic

Boundary Conditions.

As mentioned throughout this section, the proposed numerical models are:

Averaged isotropic material		
	E (GPa)	ν
Top plate (Spruce)	2.08	0.01
Back Plate (Rosewood)	5.93	0.13

Table 3.2: Elastic properties for isotropic material.

- Numerical model of bandola's top plate.

- Numerical model of bandola's back plate.

- Numerical model of bandola's enclosed air.

- Numerical model of coupled system: top plate-enclosed air.

- Numerical model of coupled system: top plate-enclosed air-back plate.

Boundary conditions are set according to phenomenon and allow the solution of the problem. Now, it is required to indicate the boundary conditions that characterize each model:

- **Top plate.** Separate top plate vibrates clamped at the edge, i.e., the transverse displacement function and its slope equal to zero, as shown in the theoretical framework.

- **Back plate.** Separate back plate also vibrates clamped at the edge.

- **Enclosed air.** The pressure at the external transverse area of the sound hole equals the atmospheric pressure. This characteristic allows the air to move in and out the cavity as in a Helmholtz resonator. The walls are considered rigid.

- **Coupled system: top plate-enclosed air.** Bandola's top plate and back plate are clamped to the ribs and they enclose the air; back plate is considered rigid but top plate vibration couples the system. Each oscillator in this coupled system has the above boundary conditions except that back plate is completely rigid. The coupling condition is present over the top plate-air interface and states that normal to the interface, fluid particle accelerations are equal to plate accelerations.

- **Coupled system: top plate-enclosed air-back plate.** This model has the same conditions presented above, but now back plate can vibrate clamped at the edge and the coupling condition is also specified for back plate-air interface.

3.2 CAD Models and FEM Simulations

3.2.1 CAD Models

CAD models were designed using SolidWorks®. According to numerical models proposed for analysis, they are presented as follows.

Top plate

Figure 3.8 presents CAD model for top plate which consists of a drop-shaped plane surface. Dimensions are specified in Figure 3.9.

As it was mentioned, simple models are pursued and hence, fan bracing, harmonic bars, bridge and sound hole reinforcement are not considered. These parts of the bandola, at low resonances, are expected to increase mass and stiffness without changing the shape modes.
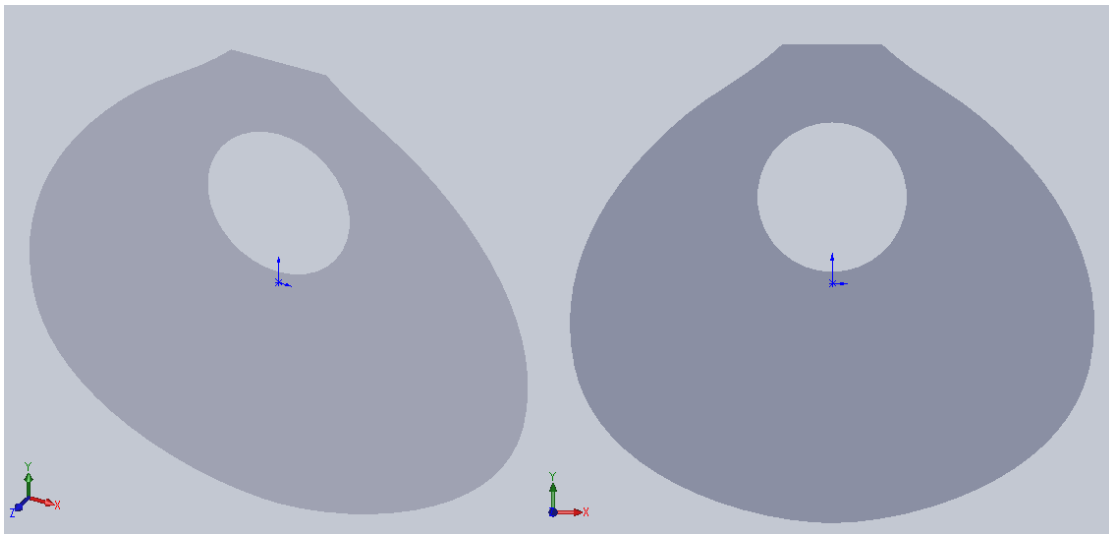

Figure 3.8: CAD model for Top plate

Back Plate

For the same reasons as for top plate, reinforcement bars are not consider into the model. Figure 3.10 presents CAD model for back plate which also consists of a drop-shaped
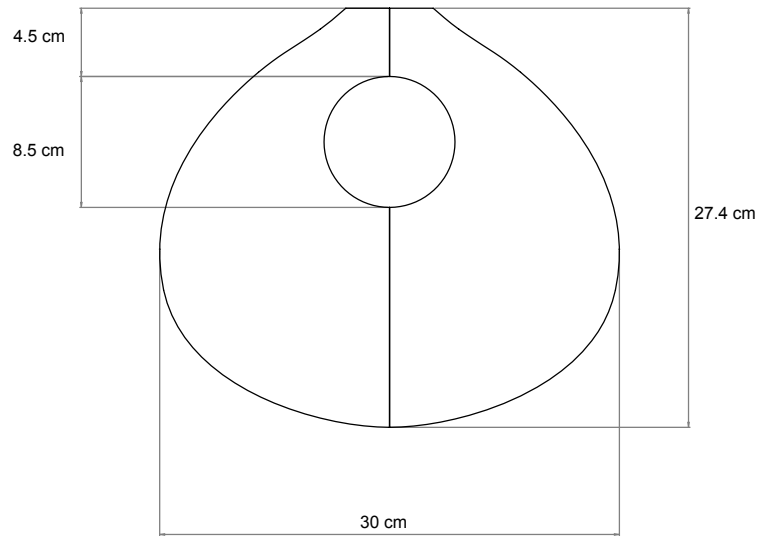
Figure 3.9: Dimensions of modelled plates

plane surface. Dimensions are the same for top plate.

Enclosed air and coupled systems

It was stated that the air inside the cavity vibrates at the first mode almost as a Helmholtz resonator. This assumption is not so simple because of the geometry of the instrument and also because the cavity walls are not completely rigid. Additionally, the concept of "length of the neck" does not refer exactly to a length determined by either end of the neck. In guitars, for example, it could be thought that the length of the plug of the air is given by top plate thickness, however, practice have shown that an extra volume both inside and outside moves with the air in the neck due to the inertia of the oscillating piston when it gets to its original position. This event is called the *end effect* and the correction that should be applied in order to consider it is related to and of similar size to the diameter of the hole, so the mass of air is substantial. Applying the the correction used for guitars, the effective length of the "plug" of air of the bandola will be about 1.7 times the radius of the hole.

The CAD model of enclosed air should represent the enclosed volume of air together with the effective length of the resonator's neck. The model presented in Figure 3.11 could represent not only the above ideas, but also the complete body, formed by surface planes for plates and enclosed volume of air, which is useful for coupling the systems.
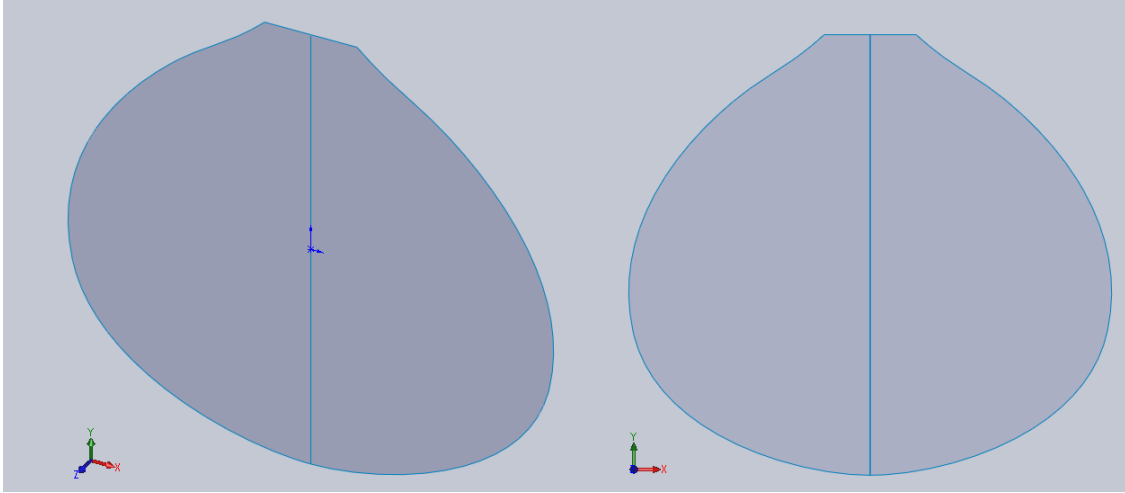
Figure 3.10: CAD model for Back plate

The ribs have a depth of 10cm as specified.

3.2.2 Considerations for FEM Simulations

Simulations were executed using the commercial software ANSYS®. The elements in ANSYS® library, used for meshing the plates and air, are presented as follows.

Element SHELL281 for plates

The analysis of plates was performed using the element SHELL281 whose formulation is based on the Mindlin-Reissner theory and hence, it is suitable for the analysis of thin to moderately-thick shell structures [65]. The element is defined by shell section information and by eight nodes (I, J, K, L, M, N, O and P) with six degrees of freedom at each node: translations in the x, y, and z axes, and rotations about the x, y, and z-axes.

Figure 3.12 shows the geometry, node locations and the element coordinate system for this element. A triangular-shaped element may be formed by defining the same node number for nodes K, L and O.

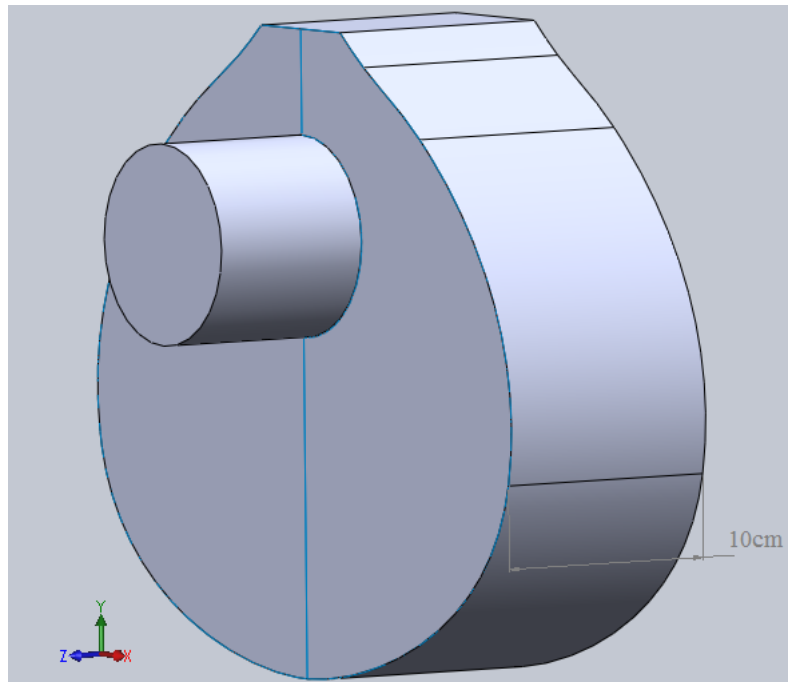A mesh for the top plate using SHELL281 is presented in Figure 3.13.

Figure 3.11: CAD model for Bandola's resonance box

Element FLUID220 for air

The element FLUID220 was used for meshing the air. This is a 3-D 20-node solid element that exhibits quadratic displacement behavior and is used for modeling the fluid medium and the interface in fluid/structure interaction problems [65].

The element formulation is based on governing equation for acoustics, namely the 3-D wave equation, and also takes into account the coupling of acoustic pressure and structural motion at the interface. The element node has four degrees of freedom per node: translations in x, y and z directions, and pressure. The displacements are only applicable at nodes that are on the interface.

Figure 3.14 shows the geometry, node locations and the coordinate system for this element.

A mesh for enclosed air using FLUID220 is presented in Figure 3.15.
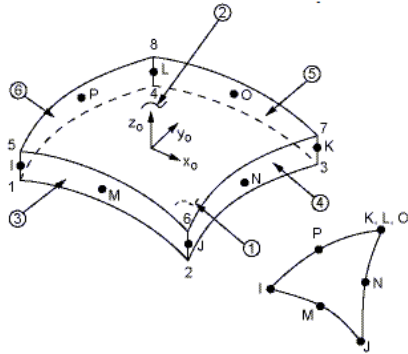
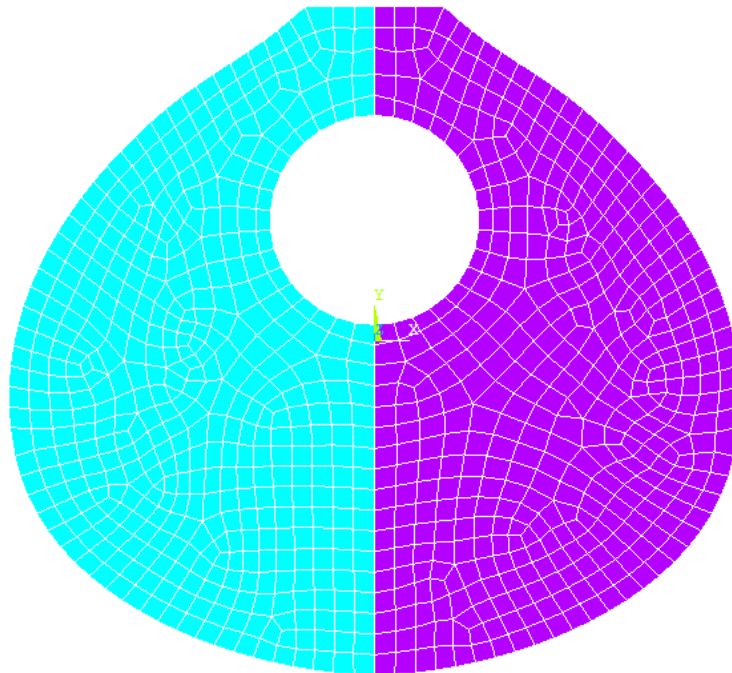**Figure 3.12:** Geometry of element SHELL281 used for meshing the plates

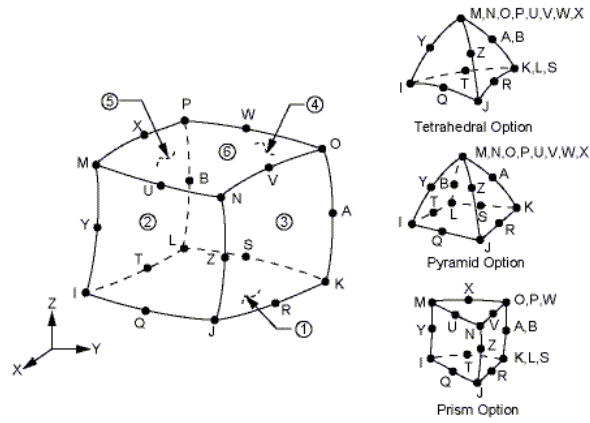**Figure 3.13:** The Top plate meshed with the element SHELL281

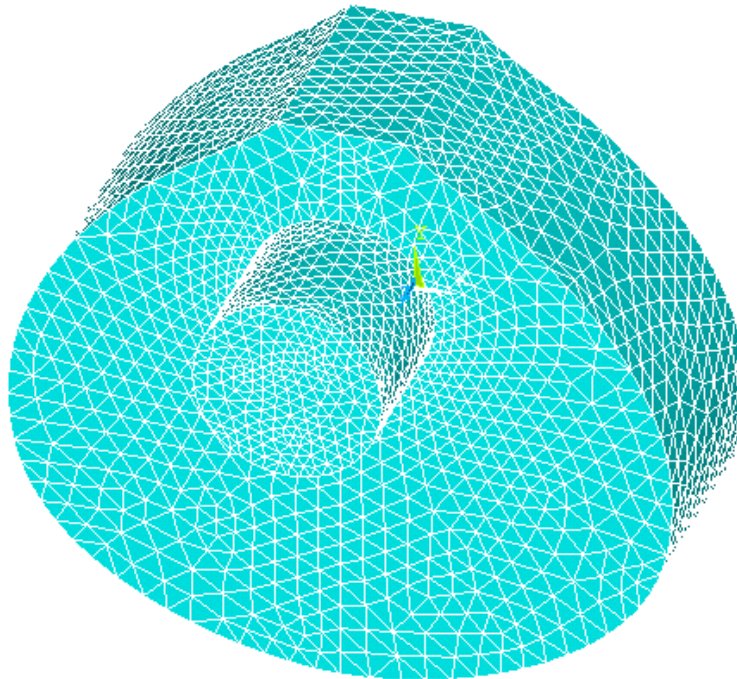**Figure 3.14:** Geometry of element FLUID220 used for meshing the air

Figure 3.15: The enclosed air meshed with the element FLUID220

Chapter 4

Results and Analysis

4.1 Modal analysis of uncoupled elements.

4.1.1 Modal analysis of top and back plates.

The analysis starts with the study of the plates, assuming spruce for top plate and rosewood for back plate and imposing clamped boundary conditions at the edge. Using a range of analysis of 0-800Hz, the six lowest modes of vibration of bandola's top and back plate are presented in Figures 4.1 and 4.2, where each mode is identified with the label (m, n) that refers to the number m, n of antinodal areas in the x and y directions respectively. Initials "T" for top plate and "B" for back plate that begin the mode label are used to specify the modes for each plate. Colored bar indicates the scale of contours displacement, ranging from blue, the minimum displacement, to red, the maximum displacement. These displacements are not an absolute quantity since each mode is normalized separately, however, their importance lies in the relation between the different contours (amplitudes) in the plate.

Computed mode frequencies are also presented in Figures 4.1 and 4.2. According to the material properties of each wood, frequency values for back plate modes are higher than those for top plate. Rosewood is a hardwood and hence, higher frequencies were expected.

By comparing the frequencies with those for open strings in Table 2.1, it can be observed that calculated frequencies of the plates are within the sound register of bandola. This fact could mean that material properties used for analysis are in a good range of
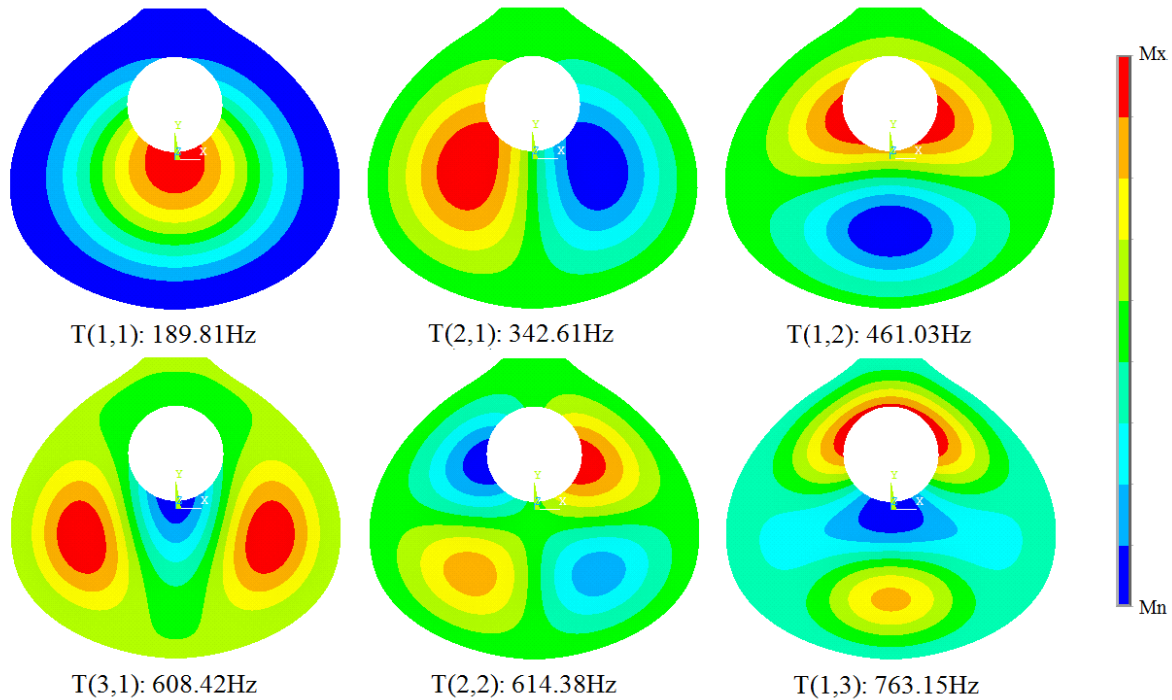
Figure 4.1: Simulated modes of vibration of the top plate.

approximation. Despite of this, it is known that fan bracing and harmonic bars have the effect of increase resonance frequencies of the plates and thus, if numerical models had considered fan bracing, harmonic bars or any structural reinforcement, the modal frequencies would have been higher. Something similar happens in classical guitars [11], where first top and back plate frequencies, usually 183Hz and 204Hz respectively, are far enough from the lowest tuning frequency of open strings, which is 82Hz.

Analyzing the resulted mode shapes for the bandola's plates, it can be confirmed, like in guitars, that the fundamental modes (1,1) are characterized by symmetrical variation of amplitude over the bout of the bandola. This result supports the assumption of coupling models based on [7, 8], where these first modes of the plates are modelled as simple harmonic oscillators that represent the displacement of the mode effective mass. Besides the fundamental modes, the others can be identified according the experimented stresses, i.e., modes (2,1) and (3,1) are recognized as "transverse flexural modes", modes (1,2) and (1,3) are the "longitudinal flexural modes", and the mode (2,2) is called the "shear mode".
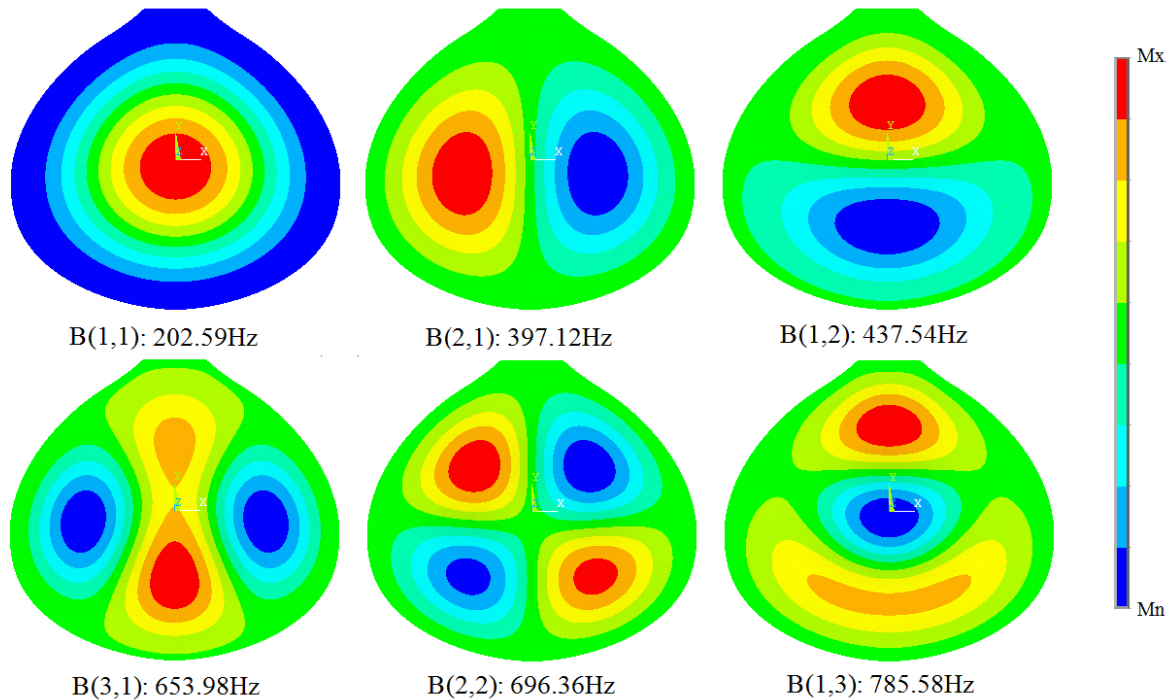
B(1,1): 202.59Hz   B(2,1): 397.12Hz   B(1,2): 437.54Hz

B(3,1): 653.98Hz   B(2,2): 696.36Hz   B(1,3): 785.58Hz

Figure 4.2: Simulated modes of vibration of the back plate.

The modes presented for bandola's plates are quite similar to guitar plate modes, as seen in Figure 2.8. The guitar top plate in the figure has fan bracing and harmonic bars, so, it could be said that the presence of these elements doesn't have a significant effect on the shapes of lower modes, as mentioned before.

4.1.2 Modal analysis of enclosed air.

Due to the substantial mass of air contained in the volume of the cavity, it is expected the computation of larger wavelengths of air pressure compared with those presented for plates. Figure 4.3 shows the obtained modes for the air in the cavity in a range of 0-800Hz, where the values of modal frequencies confirm above idea. The three lowest modes are identified as the air modes A0, A1, A2. Colored bar indicates the scale of contours pressure, ranging from blue, the minimum pressure, to red, the maximum pressure.

Air mode A0 is known as the Helmholtz resonance and according to the coupling
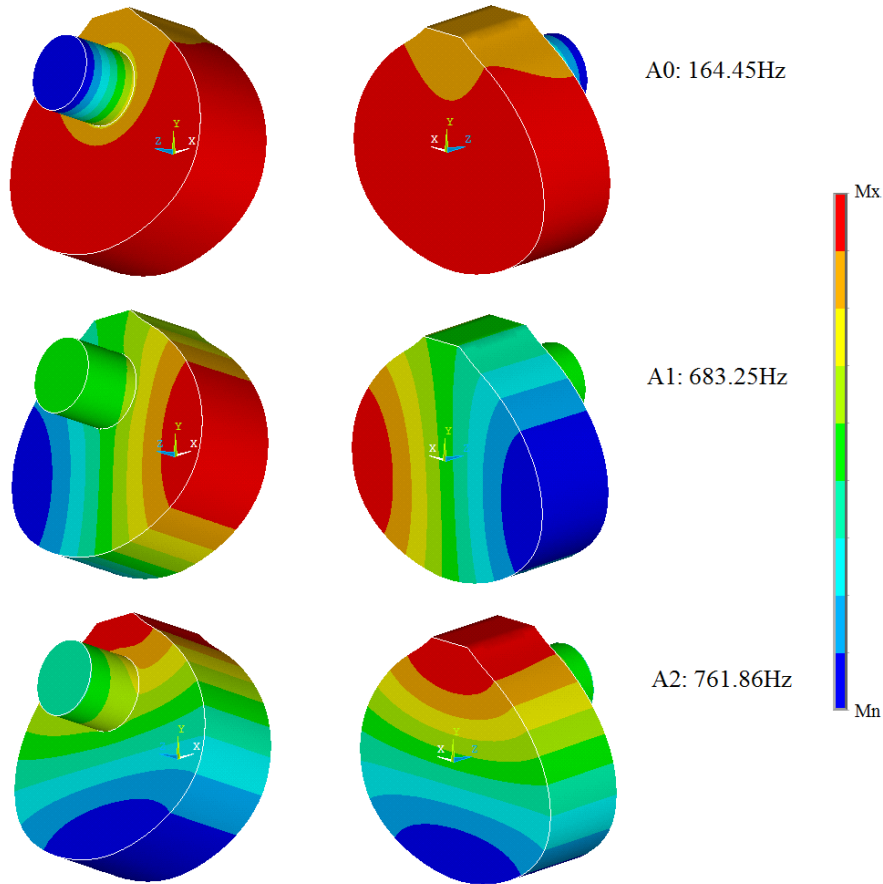
Figure 4.3: Air modes A0, A1 and A2.

models, it is of great importance for bandola's dynamic response at low frequencies since it couples the system. A pure Helmholtz resonator is characterized by a maximum constant pressure inside the cavity (that acts as an air cushion) and a pressure variation in the region of the neck that drives the oscillating piston of air. Considering this, the mode A0 presented in Figure 4.3 indicates that air inside of bandola's cavity doesn't behave exactly as a Helmoholtz resonator (though it is very similar) since it presents a little variation in pressure along the cavity. This fact could be explained considering the geometry of the bandola.

It can be observed that the frequency of A0 is considerably far apart from the other modal frequencies, constituting a difference of almost two musical octaves for the

nearest mode A1. This characteristic could reflect the great influence of this first mode at the lowest frequencies of the bandola by comparing both the obtained frequencies for plates and bandola's sound register in Table 2.1.

Besides A0, A1 shows a transverse pressure distribution similar to a half wave along the height of the bandola; and on the other hand, A2 shows a longitudinal pressure distribution similar to a half wave along the width of the bandola.

4.2   Modal analysis of coupled elements.

The dynamic response of a structure can be described in terms of the modal parameters. In this sense and according to the coupling models proposed, the normal modes of single structures combined could determine the response a complex structure formed by their assembly. With the uncoupled modes already calculated, the analysis of coupled modes is presented as follows.

4.2.1   Coupled system: Top plate - enclosed air.

Figures 4.4, 4.5 and 4.6 show the calculated modes for the system in which the top plate and the air in the cavity interact. Nine modes are presented in the range of 0-800Hz, from these modes several patterns of the uncoupled modes can be identified. The modes are labelled with the initials "TA" that indicate the coupling between Top plate and Air, the scripts "DT", "PF" and "PB" are used to specify the variable plotted, i.e., displacements in top plate, pressure in the front view and pressure in the back view, respectively. Color bar indicates the scale of contours magnitude corresponding to the plotted variable, ranging from blue, the minimum magnitude, to red, the maximum magnitude.

The uncoupled modes calculated for top plate and air have shown that Helmholtz resonance of the air A0 is lower than the fundamental resonance of the top plate T(1,1). As it is exposed in the Figure 4.4, TA(1) and TA(2) present in turn, lower and higher resonances (respectively) compared with those of uncoupled elements. With these results and according to the coupling model of two oscillators, combination of both the fundamental resonance of top plate and the Helmholtz resonance thus give rise to a lower resonance TA(1) and a higher resonance TA(2).

The mode shapes presented are very consistent with above idea: TA(1)-PF shows exactly the mode shape of A0 and TA(1)-DT can be recognized as the fundamental
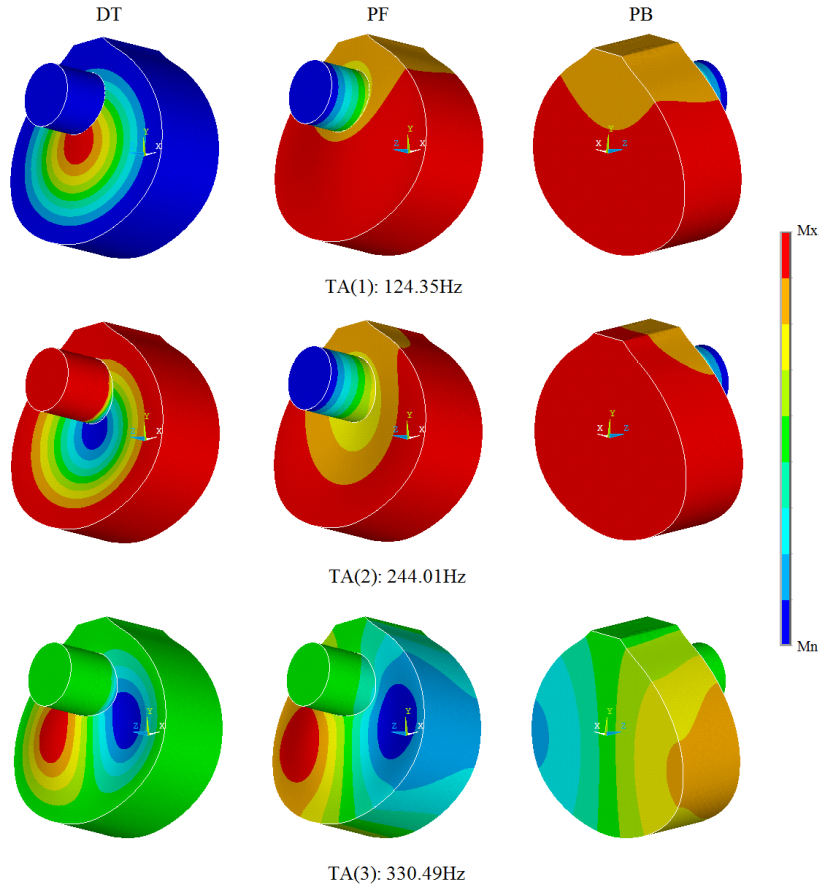
Figure 4.4: Coupled modes of vibration for bandola's resonance box considering the oscillation of top plate and enclosed air. The back plate is assumed to be rigid.

top plate resonance; moreover, TA(2)-PF is similar to A0 but not exactly the same: the pressure variation is greater throughout the cavity, on the other hand, TA(2)-DT remains very similar to T(1,1). Many authors have shown for guitars, that first coupled mode is governed mainly by the Helmholtz resonance whereas the second is governed by the fundamental resonance of the top plate [7, 11]. Using this concept, it could be thought that the great similarity between TA(1)-PF and A0 indicates the great influence of A0 in the coupled mode; and the rough similarity between TA(2)-PF and A0, indicates the low influence of A0. Therefore, it may be concluded that TA(1) is driven by the air mode and TA(2) by the structure mode. From mode shapes, it can

Figure 4.5: Coupled modes of vibration for bandola's resonance box considering the oscillation of top plate and enclosed air. The back plate is assumed to be rigid.

also be said that these two coupled modes seem to be efficient radiators since a big area of the bout of the bandola excites the air in front of it. The efficiency of this radiation will also be determined by the phase of piston air and in order to get any information of it, it would be convenient experimental measurements.

Verifying the expression in E.q.3.18 it is found that:

$$\sqrt{f_p^2 + f_h^2} = 251.14\text{Hz}$$
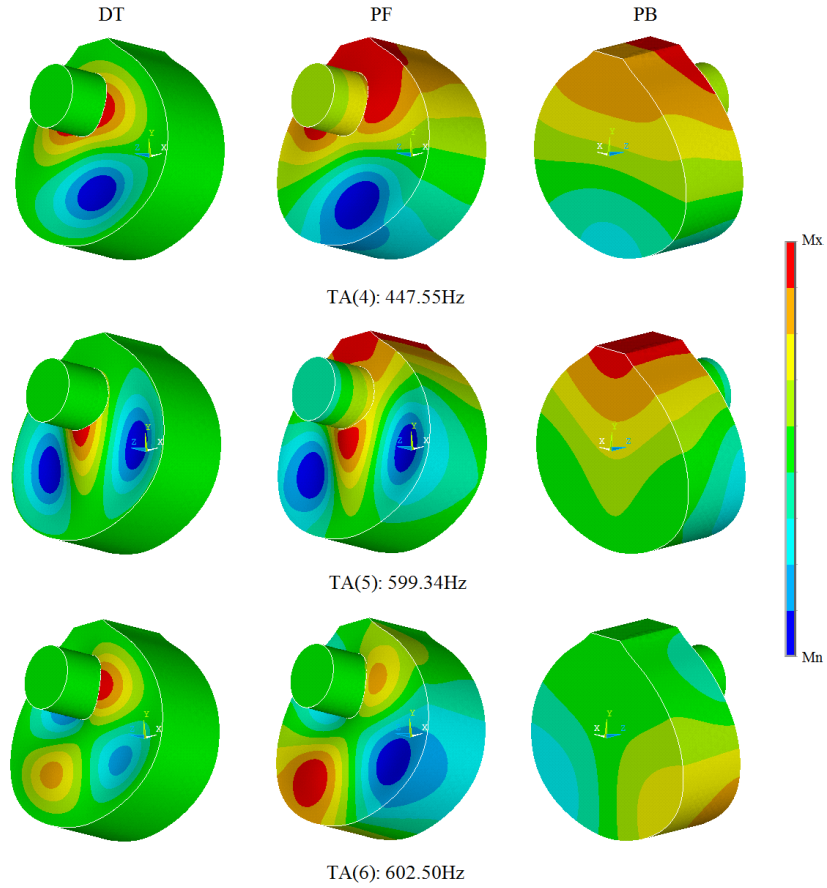$$\sqrt{f_1^2 + f_2^2} = 273.87\text{Hz},$$
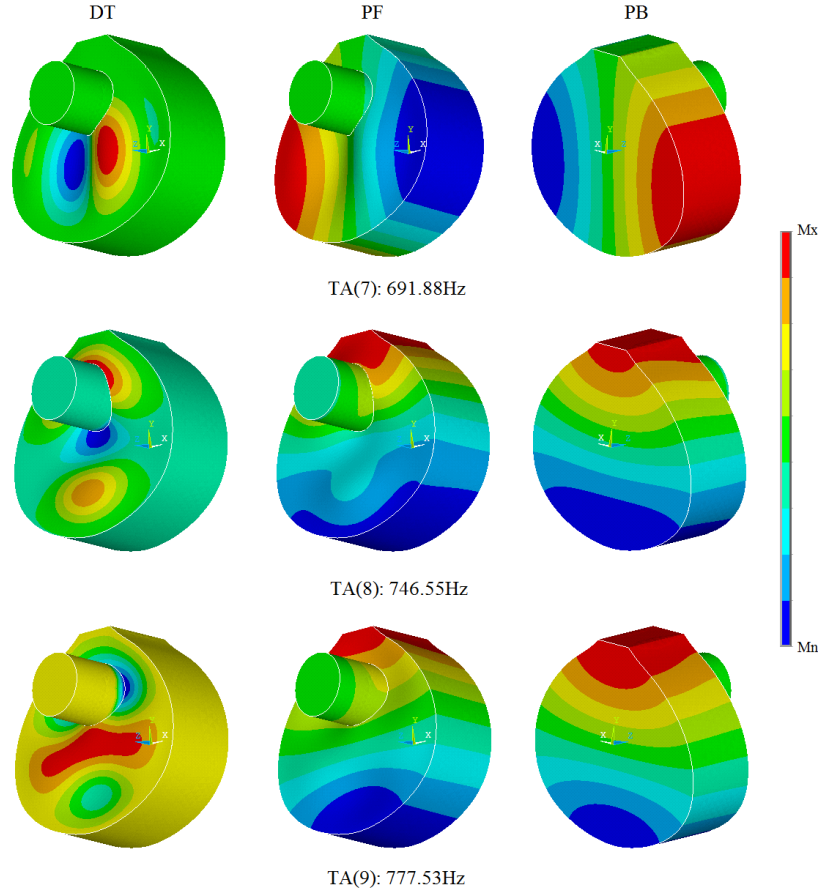
Figure 4.6: Coupled modes of vibration for bandola's resonance box considering the oscillation of top plate and enclosed air. The back plate is assumed to be rigid.

where the frequency $f = \omega/2\pi$. These results are consistent since the percent error, relative to the sum of coupled terms, is 8.3%. At this point, it would be convenient an experimental validation.

Through E.q.3.17

$$\omega_{1,2}^2 = \frac{1}{2}(\omega_p^2 + \omega_h^2) \pm \frac{1}{2}\sqrt{(\omega_p^2 - \omega_h^2)^2 + 4\omega_{ph}^4},$$

it can be noted that separation between both coupled resonance frequencies is given by the frequency difference between Helmholtz and fundamental top plate resonances, taking into account that ω_h and ω_p will always lie between ω_1 and ω_2. The coupling

term ω_{ph} will also be affected by this difference through the ratios of effective areas and masses of the oscillators:

$$\omega_{ph}^4 = (\mu SA)^2 / m_p m_a.$$

Thus, close uncoupled resonances will produce close coupled resonances whereas separate uncoupled resonances will produce even more separate coupled resonances. Since the modification of Helmholtz resonance in a bandola implies changing the dimensions of the entire resonance box, the only independently parameter that could be varied in order to control the coupling is the effective mass of the top plate.

Now, with respect to the other coupled modes in the frequency range, it can be observed that mode shapes A0 and T(1,1) are no longer recognizable. Throughout the following 7 modes, the combination of the remaining 5 modes of the plate with the other two of the air is presented. As it was expected, the resultant modes are combination of uncoupled modes. In this sense, models more complex could be considered in order to predict more modes, using more oscillators representing every mode in the plate or in the air. A model with nine oscillators, three representing the modes of air inside the cavity and six representing the modes of the top plate, all lying into the same frequency range, would predict the nine calculated coupled modes, also into the same range.

In TA(3), it can be identified the mode shapes of T(2,1) and A1. Although the frequencies of these uncoupled modes are very distant from each other, the mode TA(3), with a frequency of 330.49Hz, seems to be governed by these two modes. TA(3)-DT presents two lobes that move in anti-phase, by following the idea that the sound radiation depends on the net volume of air that is displaced, this mode seems to be not so efficient as are the first two modes. TD(3)-PF and TD(3)-PB show how the shape of TA(3)-DT influences the pressure distribution at the region near to the plate, taking gradually the form of the pressure distribution in A1 only till the back. Considering this pressure behavior and noting that the frequency of TA(3) is closer to the frequency of T(2,1), it may be inferred that this coupled mode is mainly driven by the second plate mode T(2,1).

In TA(4), the mode shapes T(1,2) and A2 can be identified and seem to govern the coupled mode. Again, T(1,2) is closer in frequency to TA(4) and influences the pressure distribution, therefore, it can be said that it drives the coupled mode. TA(5) insinuates the presence of T(3,1) and A2, and presents the same type of characteristics described above for TA(4), although the pressure distribution is not only dominated by A2 since a little distortion can be appreciated in the back view. This effect may be produced by the influence of A1.

TA(6) suggest a marked presence of the shear mode T(2,2), but the influence on pressure distribution cannot be certainly described by only one known mode, however, it may be produced by the combination of A1 and A2. Again in TA(7), the mode A1 dominates the pressure distribution and a mode very similar to T(2,1) is identified in the top plate, though TA(7)-DT presents two little lobes beside the central two big lobes. This effect may be produced by A1 and in this way, this coupled mode would be driven by A1, inversely with that described for TA(3).

Finally, both TA(8) and TA(9) seem to be governed by T(1,3) and A2, but differing in the phases of top plate displacement and in a more influence of A2 in TA(9) than in TA(8). This leads to infer that TA(8) is driven by T(1,3) and TA(9) by A2.

After these descriptions of the coupled modes, it can be mentioned some global characteristics from of all of them. First, the correspondence between uncoupled modes of the top plate and the air in every coupled mode, seems to respond to the longitudinal or transverse disposition of the modes, for instance, transverse top plate modes are usually related to the transverse pressure distribution of mode A1, whereas longitudinal top plates modes are related to the longitudinal pressure distribution of mode A2. The shear mode of the top plate also support this idea since it was related to a pressure distribution that can be described from the combination of both air modes A1 and A2. The other characteristic identified was that coupled modes may be usually driven by those uncoupled modes with the nearest frequency.

4.2.2   Coupled system: Top plate - enclosed air - back plate.

Figures 4.7, 4.8 and 4.9 show the calculated modes for the system in which the top plate, the air in the cavity and the back plate interact. Fifteen modes are presented in the range of 0-800Hz, from these modes several patterns of the uncoupled modes can be identified in the same way as the system of two oscillators just presented. The modes are labelled with the initials "TAB" that indicate the coupling between Top plate, Air and Back plate, the scripts "DT", "DB", "PF" and "PB" are used to specify the variable plotted, i.e., displacements in top plate, displacements in back plate, pressure in the front view and pressure in the back view, respectively. Colors indicate the scale of contours magnitude as in above figures.

It is observed in Figure 4.7 that TAB(1) presents clearly the same mode shapes of T(1,1) and B(1,1) in top and back plates respectively, and that A0 can be easily recognized in the pressure distribution. In this mode, top and back plate vibrate with

opposite phases, moving outward and inward and changing considerably the volume of the resonance box. Due to this motion, the air is drawn and expelled from the cavity like a breathing. TAB(1) can be thus called, as in others instruments with resonance box, the "breathing mode" [66]. Moreover, TAB(2) also presents the shapes of T(1,1) and B(1,1), however, the pressure distribution is very confusing and seems to be highly influenced by both shapes of top and back plate. This time the plates vibrate in phase and thus, the volume of resonance box will change a small amount that depends on the displacement amplitude of the plates, which in this case is greater for top plate. The third coupled mode TAB(3) doesn't have the same problem of identifying the mode that governs pressure distribution: A0 is easily recognized, although a greater pressure variation is present throughout the cavity. The mode shapes in top and back plate are also related to T(1,1) and B(1,1), but now the mode in the back plate present a bigger area of displacement. The motion between both plates is again in opposite phase.

According to the model of coupling with three oscillators, these three lowest modes TAB(1), TAB(2) and TAB(3) show the influence of mainly T(1,1), B(1,1) and A0. In each case, one of the uncoupled modes is dominant over the others, for instance, A0 drives the first coupled mode, T(1,1) drives the second and B(1,1) drives the third. Additionally, these modes seem to be efficient radiators although this is also determined by the phase of piston air. Thus, it would be convenient some experimental measurements in the bandola.

By examining TAB(1), TAB(2) and TAB(3), it can be observed that $f_1 < f_h$, $f_2 < f_p$ and $f_3 > f_b$ where $f_b > f_p > f_h$. In comparison with the two lowest modes TA(1) and TA(2) predicted by the model of two oscillators, the frequencies of TAB(1) and TAB(2) decreased in value as if the effect of considering the back plate was that of an added mass. For guitars, Meyer and Elejabarrieta [27, 41] have reported the same behavior when considering the vibration of back plate, however, Christensen [8] has clarified that the second coupled resonance TAB(2) may be moved either upward (for $f_b < f_p$) or downward (for $f_b > f_p$), depending upon the uncoupled resonance frequencies f_b and f_p of the top and back plate.

E.q.3.22 allows to conclude, as in the analysis of the system: top plate-air, that a way to control the coupling in the practice is changing the ratios between effective areas and masses, specially through the manipulation of the effective masses m_p and m_b.

Verifying the expression in E.q.3.23 it is found that:

$$\sqrt{f_p^2 + f_h^2 + f_b^2} = 322.66\text{Hz}$$
$$\sqrt{f_1^2 + f_2^2 + f_3^2} = 351.65\text{Hz}.$$

These results are consistent since the percent error, relative to the sum of coupled terms, is 8.24%. With this result, the next step would be an experimental validation, as suggested before.

The effect of considering the back plate in the coupling model is also followed in the other modes. TAB(4) presents, in the case of plates, the mode shapes of T(2,1) and B(2,1) with a displacement amplitude greater at the top plate. This top plate mode shape, in turn, seems to influence the pressure distribution which is mainly governed by A1. The case of TAB(5) is almost the same, although this time the back plate presents the dominant mode with greater amplitude, which also influences the pressure distribution. Both modes may not be good sound radiators as it was discussed, however in practice, TAB(5) could be more efficient since vibrations of back plate are damped when the instrument is played.

From this point, the next coupled modes exhibit a poor coupling between top and back plate. It can be observed how the structures are nearly motionless in all cases: the air is not able to couple the plates and therefore, the mode appear in only one of them. Furthermore, the air mode that accompanies the mode vibration, seems to be very influenced by the only plate mode governing the resonance or even non-existent. This behavior can be identified in TAB(6) and TAB(7), both composed mainly by T(1,2), B(1,2) and A2; also in TAB(8) and TAB(9), composed mainly by T(3,1), B(3,1) and A2; in TAB(10) and TAB(11), composed by T(2,2), B(2,2) and a very weak unknown air mode; and finally in TB(13), where only B(1,3) can be identified.

The mode TAB(12) presents again a considerable coupling between plates and air. A1 dominates the pressure distribution and modes very similar to T(2,1) and B(2,1) are presented in the top and back plate. TAB(14) and TAB(15) show almost motionless in back plate, but the air and the top plate are strongly coupled since it can be recognized marked modes for each of them. Thus, these modes are composed by T(1,3) and A2, dominating T(1,3) in TAB(14) and A2 in TAB(15).

By observing all coupled modes that were calculated, it is noted that the combination of the uncoupled modes of the plates and the air produces the coupled modes, all lying into the frequency range of 0-800Hz. However, only at the lowest five modes is

achieved a strong coupling between the modes of the top plate, the enclosed air and the back plate. The rest of the modes could present a coupling between the top plate and the air alone or almost vibrate separately. This coupling could be thought to have a repulsive effect on the modes with increasing frequency.

Dynamic response (into a specific frequency range) of a complex structure may be described by the combination of the modes of each substructure (all lying in the same frequency range) [61], therefore, a model considering fifteen uncoupled oscillators, three representing the modes of air inside the cavity, six representing the modes of the top plate and other six for the modes of the back plate, could predict the fifteen calculated coupled modes.

Figure 4.7: Coupled modes of vibration for bandola's resonance box considering the oscillation of top plate, enclosed air and back plate

DT   DB   PF   PB

TAB(6): 380.24Hz

TAB(7): 448.11Hz

TAB(8): 577.54Hz
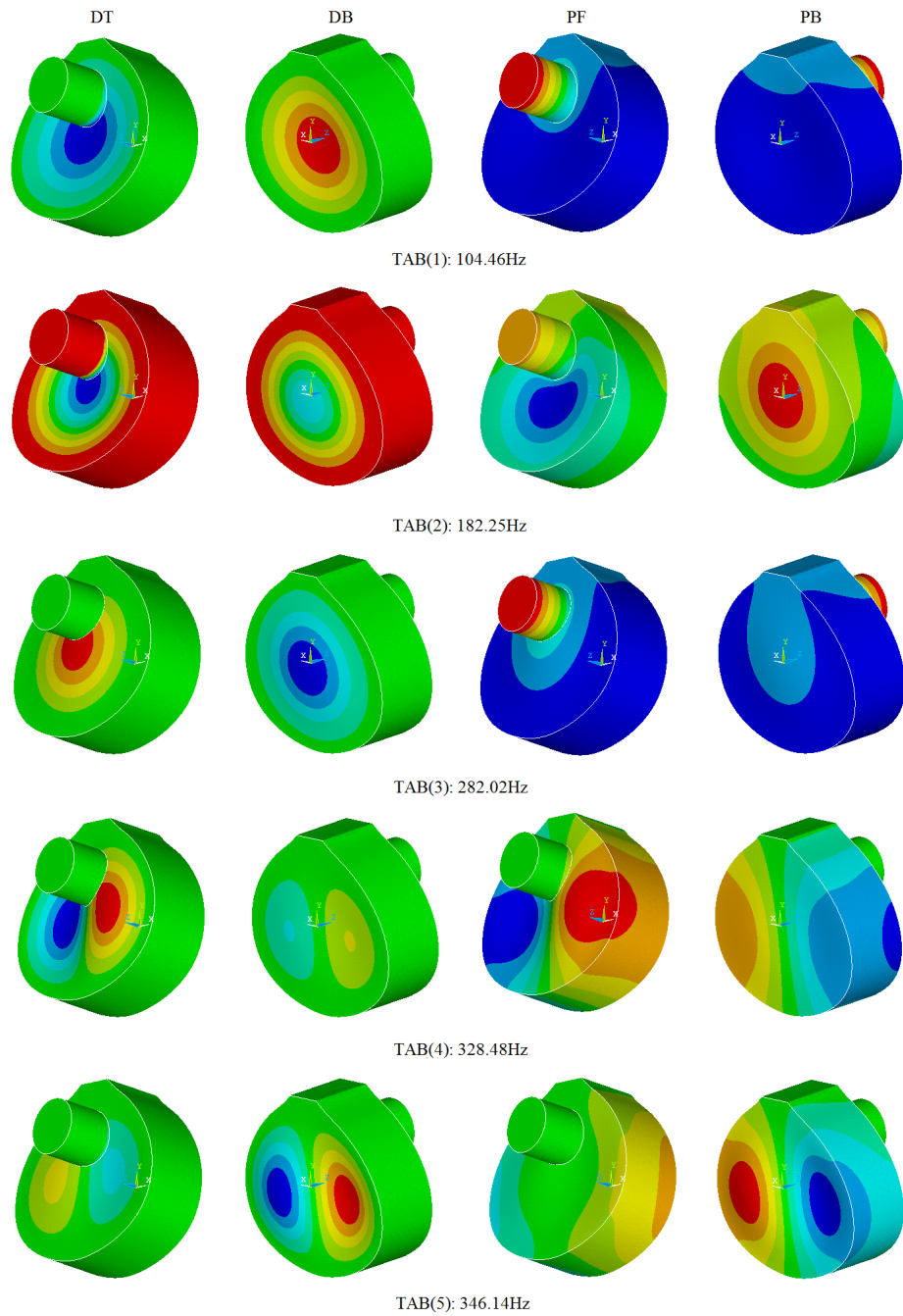
TAB(9): 599.49Hz

TAB(10): 602.05Hz

Figure 4.8: Coupled modes of vibration for bandola's resonance box considering the oscillation of top plate, enclosed air and back plate

73

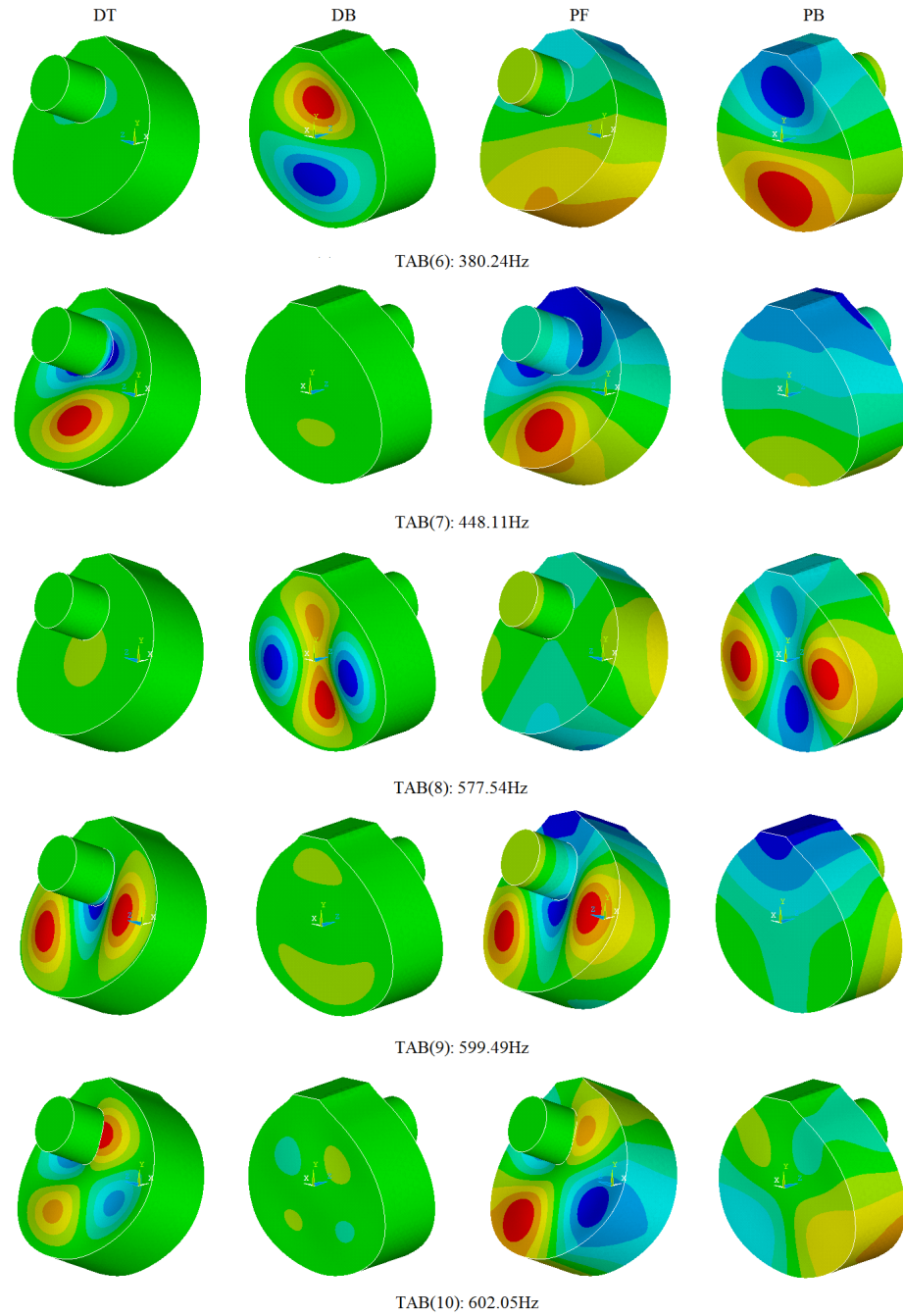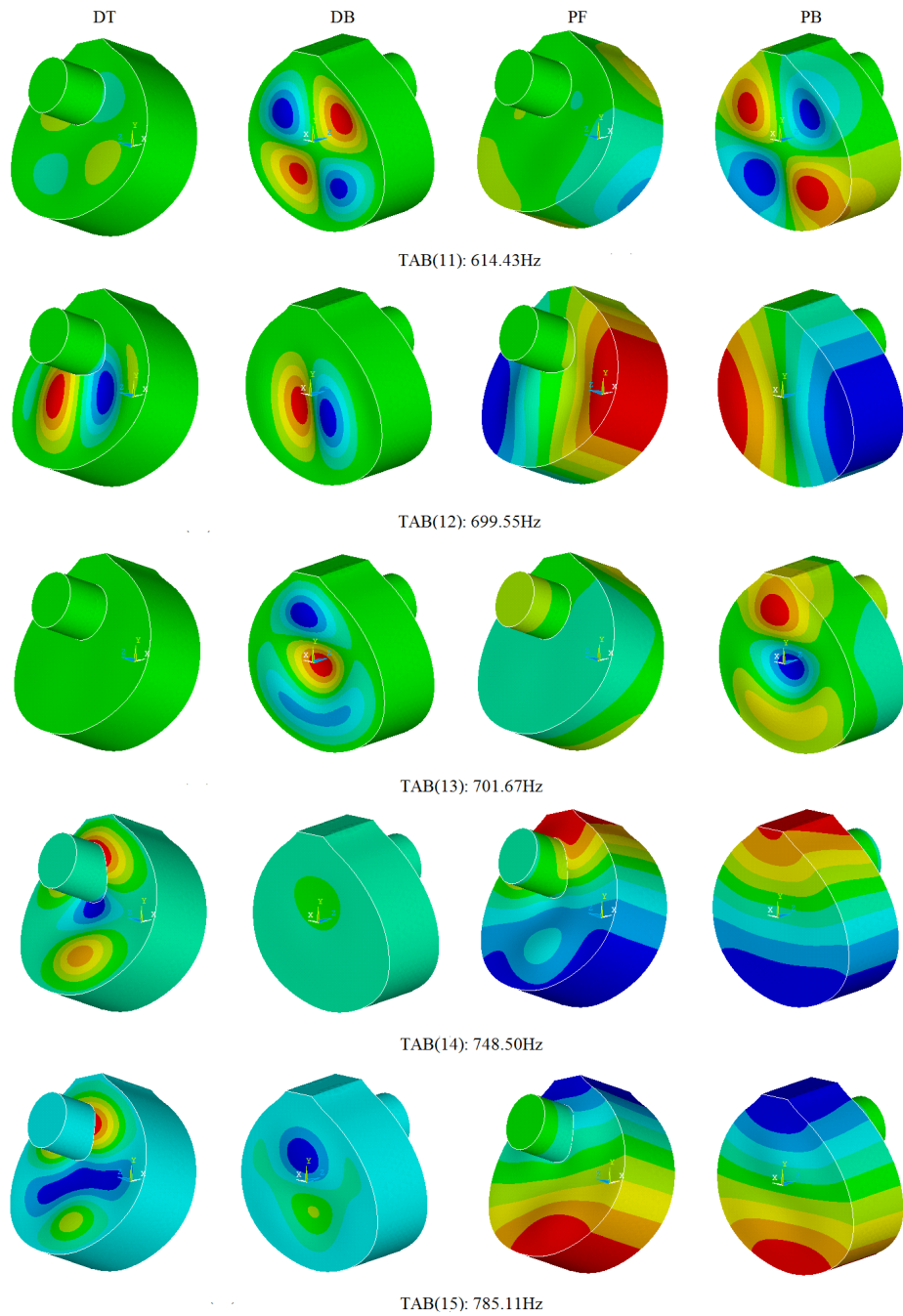**Figure 4.9:** Coupled modes of vibration for bandola's resonance box considering the oscillation of top plate, enclosed air and back plate

Chapter 5

Conclusions

The analysis of modal coupling at the frequency range of 0-800Hz in a Colombian Andean Bandola in C was performed using the Finite Element Method. First, the coupling was described for two cases using coupled systems with two and three oscillators. This allows one to validate the numerical analysis developed later, where it was verified the coupling between each first uncoupled mode of the top plate, the enclosed air and the back plate, at the lowest two and three resonances (depending on the case) of the coupled systems. The rest of the computed modes were also combinations of other uncoupled modes of each element.

The methodology developed to tackle the problem was useful for the understanding of the dynamic behavior of the bandola. The analysis based on the coupling phenomenon (described by coupled oscillators) allows identifying the influence of the uncoupled modes on the resultant coupled modes. In each case one of the uncoupled modes is dominant over the others. The coupled systems that were studied allowed identifying a way to control the coupling in the practice; changing the ratios between effective areas and masses, especially through the manipulation of the effective masses of the plates. As a general conclusion of the analysis, the coupled system of top plate-enclosed air presented a strong coupling in all the nine coupled modes. Nevertheless, in the coupled system of top plate-enclosed air-back plate the coupling could be thought to have a repulsive effect on the modes with increasing frequency.

Finally, it is important to mention that in the range of 0-800Hz six modes were found for the top and back plate and three for the enclosed air. For the coupled systems: top plate-enclosed air and top plate-enclosed air-back plate, nine and fifteen coupled modes, respectively, were found in the same frequency range. Considering that

dynamic response of a structure can be described in terms of the modal parameters, and noting that the models of coupled systems of two and three degrees of freedom predicted the response at the lowest two and three coupled modes, it could be said that the dynamic behavior of the bandola at the frequency range of 0-800Hz could be described by a model consisting of n degrees of freedom, which represent the normal modes presented for each uncoupled element at the same frequency range. This idea agrees with the theory of modal analysis [61].

In order to verify the obtained results and get more information about some characteristics of the coupled modes, for instance, the phase of vibration of the air mode and the radiation efficiency, experimental measurements are suggested as further work.

Bibliography

[1] M. Bernal. *Cuerdas más, cuerdas menos: una visión del desarrollo morfológico de la bandola andina colombiana*. Bogotá: Universidad Pedagógica Nacional, 2003.

[2] S. E. Rodríguez. *Planteamiento de una metodología de medida acústica en la bandola andina colombiana*. Medellín: Internal report of the course "Advanced Project I", Universidad EAFIT, 2010.

[3] S. E. Rodríguez. *Caracterización acústica de la afinación y los modos normales de vibración en bandolas colombianas*. Medellín: Internal report of the course "Advanced Project II", Universidad EAFIT, 2010.

[4] D. L. Brown and R. J. Allemang. *The modern era of experimental modal analysis*. Sound and vibration, 40th Anniversary Issue, 2007.

[5] G. Weinreich. *Musical Acoustics in the Twentieth Century*. Acoustical Society of America, Vol.75, 2004.

[6] G. Caldersmith. *Plate fundamental coupling and its musical importance*. Catgut Acoust. Soc. Newsletter, Vol.36, 1981.

[7] O. Christensen and B. B. Vistisen. *Simple model for low-frequency guitar function*. Catgut Acoust. Soc. Newsletter, pp.21-27, Vol.36, 1981.

[8] O. Christensen. *Qualitative models for low frequency guitar function*. J. Guitar Acoust., pp.10-25, Vol.6, 1982.

[9] F. T. Dickens. *Analysis of the first and second vibration modes in a guitar using an equivalent electrical circuit*. Catgut Acoust. Soc. Newsletter, pp.18-21, Vol.35, 1981.

[10] I. M. Firth. *Physics of the guitar at the Helmholtz and first top-plate resonances.* J. Acoust. Soc. Am., pp.588-593, Vol.61, 1977.

[11] N. H. Fletcher and T. D. Rossing. *The physics of musical instruments.* Second Edition. Springer, 2010.

[12] T. D. Rossing, J. Popp, D. Polstein. *Acoustical response of guitars.* Proc. SMAC 83. Royal Swedish Academy of music, Stockholm. pp.311-332.

[13] R. E. Ross, T. D. Rossing. *Plate vibrations and resonances of classical and folk guitars.* J. Acoust. Soc. Am., Vol.65, 72, 1979.

[14] E. V. Jansson. *Acoustical properties of complex cavities and measurements of resonance properties of violin-shaped and guitar-shaped cavities.* Acustica, Vol.37, No.4, pp.211-221, 1977.

[15] E. V. Jansson. *A study of the acoustical and hologram interferometric measurements on the top plate vibrations of a guitar.* Acustica, pp.95-100, Vol.25, 1971.

[16] G. A. Knotta, Y. S. Shinb and M. Chargin. *A modal analysis of the violin.* Journal of the Acoustical Society of America, Vol.113, No.3, pp.269-279, 1989.

[17] K. D. Marshall. *Modal analysis of a violin.* Journal of the Acoustical Society of America, Vol.77, pp.695-709, 1985.

[18] J. Meyer. *Verbesserung der Klangqualitat von Gitarren aufgrund systematischer Untersuchungen ihres Schwingungsverhaltens (Improvement of the sound quality of guitars due to systematic investigations of their vibrating behaviors).* s.l.: PTB-Report, Forschungsvorhaben , 4490, 1980.

[19] J. Meyer. *Die Abstimmung der Grundresonanzen von guitarren.* Das Musikinstrument, Vol.23, pp.179-86; English translation in J. Guitar Acoustics, No.5, 19 (1982).

[20] R. R. Boullosa. *The use of transient excitation for guitar frequency response testing.* Catgut Acoust. Soc. Newsletter, Vol.36, pp.17-20; 1981.

[21] B. E. Richardson and G. W. Roberts. *The adjustment of mode frequencies in guitars: A study by means of holographic interferometry and finite element analysis.* SMAC'83 Publication of the Royal Swedish Academy of Music, Vol.2, No.46:2, pp.285-302, 1985.

[22] A. Runnemalm and N. E. Molin. *Air cavity modes in sound boxes recorded by TV holography*. Proceedings of the 2nd Convention of the European Acoustics Association: Forum Acusticum, 1999.

[23] K. A. Stetson. *On modal coupling in string instrument bodies*. Journal of Guitar Acoustics, Vol.3, pp.23-29; 1981.

[24] M. E. McIntyre, J. Woodhouse *The Acoustics of Stringed Musical Instruments*. Interdisciplinary Science Reviews, Vol.3, 2, pp.157-173, 1978.

[25] J. A. Torres, R. R. Boullosa *Identificación a simple vista de patrones de vibración de una tapa de guitarra*. Acústica, Universidad de Coimbra, Portugal, 2008.

[26] J. A. Torres *Modos de vibracíon simulados por computadora y experimentales de una tapa de guitarra en sus etapas de construccíon*. Master Thesis, Universidad Nacional Autónoma de México, 2006.

[27] M. J. Elejabarrieta, A. Ezcurra, and C. Santamaría. *Coupled modes of the resonance box of the guitar*. s.l.: Acoust. Soc. Am., Vol. 111., No.5, pp. 2283-2292, 2002.

[28] R. R. Boullosa, F. O. Bustamante and L. A. PÃ©rez. *Tuning characteristics, radiation efficiency and subjective quality of a set of classical guitars*. Applied Acoustics, Vol.56, pp.183-97, 1999.

[29] R. R. Boullosa. *Vibration measurements in the classical guitar*. Applied Acoustics, Vol.62, pp.311-322, 2002.

[30] M. French. *Structural modification of stringed instrument*. Mechanical Systems and Signal Processing, Vol.21, pp.98-107, 2007.

[31] G. Caldersmith. *Designing a Guitar Family*. Applied Acoustics, Vol.46, pp.3-17, 1995.

[32] C. M. Hutchins. *Acústica de las tablas del violín*. Investigación y Ciencia, pp.54-64, 1981.

[33] H. L. Schwab. *Finite element analysis of a guitar soundboard I*. Catgut Acoust. Soc. Newsletter, Vol.24, pp.13-15, 1975.

[34] K. J. Bathe *Finite Elements Procedures*. Prentice Hall, Inc., 1996. ISBN 0-13-301458-4.

[35] J. Bretos , C. Santamaría and J. A. Moral. *Vibrational patterns and frequency responses of the free plates and box of a violin obtained by finite element analysis*. J. Acoust. Soc. Am., Vol.105, pp.1942-1950, 1999.

[36] E. Bécache, A. Chaigne, G. Derveaux and P. Joly. *Numerical simulation of a guitar*. Computers and Structures, Vol.83, pp.107-126, 2005.

[37] E. Bécache, G. Derveaux and P. Joly. *An Efficient Numerical Method for the Resolution of the Kirchhoff-Love Dynamic Plate Equation*. Wiley InterScience - Wiley Periodicals, Inc. Numer Methods Partial Differential Eq., Vol.20, 2004.

[38] G. Derveaux, A. Chaigne, P. Joly and E. Bécache. *Time-domain simulation of a guitar: Model and method*. Acoust. Soc. Am., Vol.20, No.6, pp.3368-3383, 2003.

[39] I. Curtu, M. D. Stanciu, C. Itu and R. Grimberg. *Numerical modelling of the acoustic plates as constituents of stringed instruments*. Tallinn, Estonia: 6th International DAAAM Baltic Conference, 2008.

[40] I. Curtu, M. D. Stanciu and N. C. Cretu. *Modal Analysis of Different Types of Classical Guitar Bodies*. Proc. 10th WSEAS International Conference on Acoustics and Music: Theory and Applications, 2009. ISBN: 978-960-474-061-1.

[41] A. Ezcurra, M. J. Elejabarrieta and C. Santamaría. *Fluid-structure coupling in the guitar box: numerical and experimental comparative study*. Applied Acoustics, Vol.66, No.4, pp.411-425, 2005.

[42] M. J. Elejabarrieta, A. Ezcurra and C. Santamaría. *Evolution of the vibrational behavior of a guitar soundboard along successive construction phases by means of the modal analysis technique*. J. Acoust. Soc. Am., Vol.108, pp.369-378, 2000.

[43] M. J. Elejabarrieta, A. Ezcurra and C. Santamaría. *Vibrational behavior of the guitar soundboard analyzed by the finite element method*. Acust. Acta Acust., Vol.87, pp.128-136, 2001.

[44] M. J. Elejabarrieta, A. Ezcurra and C. Santamaría. *Air cavity modes in the resonance box of the guitar: the effect of the sound hole*. J. Sound Vib., Vol.252, No.3, pp.584-590, 2002.

[45] M. J. Elejabarrieta, C. Santamaría and A. Ezcurra. *Estudio de la tapa armónica de la guitarra por el método de elementos finitos*. Formula, Vol.5, pp.7-37, 1999.

[46] Y. Y. Hung, S. Y. Hung, Y. H. Huang, L. Liu, and S. P. Ng *Hybrid holographic-numerical method for modal analysis of complex structures*. Optics and LaserTechnology, Vol.42, pp.237-242, 2010.

[47] O. Inã¡ciot, J. Antunes and M.C.M. Wright. *Computational modelling of string-body interaction for the violin family and simulation of wolf notes*. Journal of Sound and Vibration, Vol.310, pp.260-286, 2008.

[48] Y. H. KIM and S. M. KIM. *Solution of coupled acoustic problems: a partially opened cavity coupled with a membrane and a semi-infinite exterior field*. Journal of Sound and Vibration, Vol.254, No.2, pp.231-244, 2002.

[49] B. E. Richardson, G. W. Roberts and G. P. Walker. *Numerical model of two violins plates*. J. Catgut Acoust. Soc., Vol.47, pp.12-16, 1987.

[50] C. Staforelli, M. M. Razeto and R. Pascual. *Numerical and experimental analysis on the dynamic behaviour of the violin plates*. Proceedings of the 2002 International Conference on Noise and Vibration Engineering, ISMA, 2002.

[51] S. Takeshi and O. Teruoaki. *Classical guitar top board design by finite element method modal analysis based on acoustic measurements of guitars of different quality*. Acoust. Soc. Japan-Acoust. Sci. and Tech., Vol.29, No.6, 2008.

[52] J. A. Torres. *Exploración de Deformaciones y Radiación Sonora de una Tapa de Guitarra Usando Modelos 3D*. Querétaro: CICATA, Vol.3, No.1, 2010.

[53] J. A. Torres and R. R. Boullosa. *Influence of the bridge on the vibrations of the top plate of a classical guitar*. Applied Acoustics, Vol.70, pp.1371-1377, 2009.

[54] J. A. Torres. P. Rendón and R. R. Boullosa. *Complex modes of vibration due to small-scale damping in a guitar top-plate*. Journal of Applied Research and Techonology, Vol.8, No.1, pp.144-152, 2010.

[55] A. Benade. *Fundamentals of Musical Acoustics*. Dover Publications, 1990. ISBN 048626484X.

[56] V. Bucur. *Acoustics of wood*. Second Edition. Springer, 2006. ISSN 1431-8563.

[57] S. Chakraverty. *Vibration of plates.* CRC Press, Taylor and Francis Group. 2009.

[58] S. P. Timoshenko and J. N. Goodier. *Theory of Elasticity.* McGraw-Hill Book Co., 3rd Edition, 1970.

[59] A. W. Leissa and M. S. Qatu. *Vibrations of continuous systems.* MacGraw-Hill, 2011.

[60] O. C. Zienkiewicz, R. L. Taylor & J. Z. Zhu. *The Finite Element Method. Its basis and fundamentals.* Coupled Systems. Sixth Edition. Elsevier, 2005.

[61] D. J. Ewins *Modal Testing: Theory, practice and application.* Second Edition. Research Studies Press LTD, 2000. ISBN 0 86380 218 4

[62] M. Richardson *Modal analysis using digital test systems.* Hewlett Packard Company, Santa Clara California.

[63] M. J. García *Lecture notes on numerical analysis.* Department of Mechanical Engineering, Universidad EAFIT, 2011.

[64] J. Wolfe. *Helmholtz Resonance.* http://www.phys.unsw.edu.au/jw/Helmholtz.html. 2012.

[65] ANSYS, Inc. *ANSYS Mechanical APDL analysis guide.* Release 13.0. November 2010.

[66] D. A. Russell. *Acoustics and Vibration of Guitars.* http://www.acs.psu.edu/drussell/guitars/index.html. 2012.

[67] M. Schleske. *Meisteratelier fur Geingenbau.* http://www.schleske.de/ 2012.

[68] S. E. Rodríguez. *Acústica de la Jarana Jarocha.* México D.F.: Professional practicum internal report, UNAM - Universidad EAFIT, 2011.

[69] J. W. S. Rayleigh. *Theory of Sound.* Vol I-II. MacMillan, 1894. ISBN: 0486602923.

[70] H. Helmholtz. *On the Sensations of Tone.* Courier Dover Publications, 1954.